

189114

61

57p
; MTP-AERO-63-21)
March 4, 1963

4 ref

N68 23031

CODE-1

GEORGE C. MARSHALL

**SPACE
FLIGHT
CENTER**

HUNTSVILLE, ALABAMA

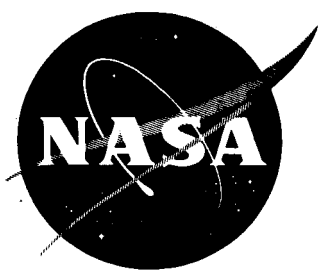
(NASA TML 50X814)

[7]

**A DUAL RATE GYRO APPROACH TO
THE ELASTIC FEEDBACK PROBLEM**

By

Robert C. Lewis
and
Thomas E. Carter



NATIONAL AERONAUTICS AND SPACE ADMINISTRATION

PRICES SUBJECT TO CHANGE

GEORGE C. MARSHALL SPACE FLIGHT CENTER

MTP-AERO-63-21

A DUAL RATE GYRO APPROACH TO
THE ELASTIC FEEDBACK PROBLEM

ROBERT C. LEWIS

and

THOMAS E. CARTER

ABSTRACT

23031

The use of ordinary filtering techniques to suppress structural feedback through control systems of large, flexible, space boosters leads to a difficult stabilization problem. This report presents a different approach to the problem through the use of dual rate gyros and a special bending filter. This dual rate-gyro concept is different from conventional methods in the following way: By subtracting the outputs of two rate gyros at different locations on the vehicle axis, the rigid body mode is eliminated from the total rate gyro signal. This resultant signal which still contains bending information passes into the special bending filter where it is divided into separate bending mode components. These separate bending mode components are then weighted and fed into the control loop to phase or gain stabilize the elastic vibrations.

The purpose of this report is to present this dual rate gyro stabilization concept and to demonstrate its application using a simplified booster model. Basic trends which provide insight into the operation of the system are determined by a simplified analysis which assumes decoupled modes. From this analysis, approximate stability bounds for gains and gyro locations can be determined.

Two possible applications of the concepts are discussed. In the first case a linear bending filter is analyzed with a representative elastic booster. In the second case an adaptive bending filter is used with the same vehicle model. In both cases stability was achieved for the nominal vehicle configuration and for 100% increase in bending mode slopes. The adaptive system was stable up to $\pm 25\%$ variation in first bending mode frequency and $\pm 40\%$ variation in second bending mode frequency.

GEORGE C. MARSHALL SPACE FLIGHT CENTER

MTP-AERO-63-21

March 4, 1963

A DUAL RATE GYRO APPROACH TO
THE ELASTIC FEEDBACK PROBLEM

by

Robert C. Lewis

and

Thomas E. Carter

DYNAMICS ANALYSIS BRANCH
AEROBALLISTICS DIVISION

DEFINITION OF SYMBOLS

SYMBOL	DEFINITION
a_o	pitch attitude gain factor
a_1	pitch rate gain factor
$A(S)$	transfer function of actuator
b_o	angle of attack gain factor
$B(S)$	transfer function of bending filter
B_1	first band pass filter of bending filter
B_2	second band pass filter of bending filter
C_1	aerodynamic moment coefficient
C_2	engine torque moment coefficient
$F(S)$	transfer function of conventional filter
$F(t)$	forcing function in a nonlinear bending equation
$F(\dot{\eta})$	a function of $\dot{\eta}$
$\frac{F-X}{m}$	longitudinal acceleration of vehicle
$g(\dot{\eta})$	nonlinear damping coefficient
j	$= \sqrt{-1}$
K_F	gain factor of conventional filter
K_1	gain factor of first band pass filter
K_2	gain factor of second band pass filter

TABLE OF CONTENTS

	<u>Page</u>
I. INTRODUCTION.....	1
II. PROBLEM STATEMENT.....	2
III. METHOD OF APPROACH.....	3
A. Preliminary Design Concepts.....	5
1. Derivation.....	5
2. Stability Bounds.....	10
3. Adaptive Stabilization.....	14
B. Application of the Concepts.....	17
1. Stabilization Philosophy.....	17
2. Basic Equations.....	20
IV. RESULTS.....	23
A. The Linear System.....	23
B. The Adaptive System.....	29
V. CONCLUSIONS.....	30
REFERENCES.....	32
APPROVAL.....	48
DISTRIBUTION.....	49

DEFINITION OF SYMBOLS

SYMBOL	DEFINITION
L_{η}	magnitude of bending mode limit cycle
m	mass of vehicle
M_B	modal mass of a general bending mode
M_1	overshoot ratio of K_1 $M_1 = \frac{K_{1 \text{ max}} - K_{1 \text{ steady-state}}}{K_{1 \text{ steady-state}}}$
M_2	overshoot ratio of K_2 $M_2 = \frac{K_{2 \text{ max}} - K_{2 \text{ steady-state}}}{K_{2 \text{ steady-state}}}$
n	subscript denoting number of bending mode
N_{α}	slope of aerodynamic normal force with respect to angle of attack
N_{β}	slope of thrust normal force with respect to engine deflection
$P_{\eta 1}, P_{\eta 2}$	peak amplitudes of first and second bending modes, respectively
R_A	magnitude of $A_1(S)$
R_B	magnitude of $B(S)$
\bar{R}_B	a stability bound of R_B
R_B^{\min}	minimum value of \bar{R}_B with respect to ϕ_B
R_F	magnitude of $F(S) A(S)$
R_o	initial value of R_B for the adaptive system
S	Laplace operator
t	time

DEFINITION OF SYMBOLS

SYMBOL	DEFINITION
V	velocity along trajectory
Y_{β}	deflection of general bending mode at engine swivel point
Y_v	deflection of general bending mode at angle-of-attack vane location
Y'_v	slope of general bending mode at angle-of-attack vane location
Y'_p	slope of general bending mode at position gyro location
Y'_1	slope of general bending mode at first rate gyro location
Y'_2	slope of general bending mode at second rate gyro location
Z	distance normal to undisturbed trajectory in pitch plane

DEFINITION OF SYMBOLS (Cont'd)

SYMBOL	DEFINITION
α_R	rigid body angle-of-attack
α_v	vane angle-of-attack reading
α_w	angle of attack due to wind
β	engine deflection angle
β_B	component of β due to bending dynamics
β_R	component of β due to rigid body dynamics
β_c	engine deflection command signal
ζ	damping ratio
ζ_F	damping ratio of conventional filter
ζ_B	damping ratio of bending mode
η	a general bending mode deflection
κ_1, κ_2	constants to be used in adaptive gain logics
σ	real part of S
σ'	closed loop damping factor of a general bending mode
τ_1, τ_2	time constants used in adaptive gain logics
φ_p	pitch attitude gyro output
φ_R	rigid body pitch attitude error
$\dot{\phi}_1$	first rate gyro output

DEFINITION OF SYMBOLS (Cont'd)

SYMBOL	DEFINITION
$\dot{\phi}_2$	second rate gyro output
$\dot{\phi}_{ba}$	bending adjustment from bending filter
$\dot{\phi}_b$	$= \dot{\phi}_1 - \dot{\phi}_2$
$\dot{\phi}_{B1}$	output of first band-pass filter in bending filter
$\dot{\phi}_{B2}$	output of second band-pass filter in bending filter
\emptyset_A	phase of $A_1(s)$
\emptyset_B	phase of $B(s)$
\emptyset_F	phase of $F(s) A(s)$
ω	imaginary part of S
ω'	closed loop damped frequency of a general bending mode
ω_B	natural frequency of bending mode
ω_F	break frequency of conventional filter
ω_{1A}, ω_{1B}	break frequencies in first band-pass filter
ω_{2A}, ω_{2B}	break frequencies in second band-pass filter

SECTION I. INTRODUCTION

A problem associated with the control of large space boosters is the stabilization of structural feedback. When elastic bending modes are sensed with the state variables and reinforced through the control system, instability results. Conventional approaches to the problem have been through direct filtering of the state variables and judicious sensor placement to gain and phase stabilize the bending modes. These techniques have been quite satisfactory for smaller ballistic missiles, but for large vehicles such as the Saturn or Nova, the bending frequencies are so low that direct filtering of the measured state variables produces either phase lag and distortion of rigid body signals, or very limited regions for acceptable sensor locations.

This report presents a different approach to the usual gain and phase stabilization techniques. The basic difference in this solution technique is that by subtraction of signals from two rate gyros, the rigid body control mode is eliminated from the bending signal. This pure bending signal which remains is then passed through a special purpose filter where the separate modes are decoupled and multiplied by appropriate gains and used in the control equation to prevent reinforced elastic vibrations. Since the special bending filter operates only on a pure bending signal, it does not affect the phase of rigid body, or other, signals. Proper selection of bending filter gains reduces the coupling between bending modes as well as the requirements to vary sensor locations for acceptable stability regions. Selection of these gains can be accomplished by a root locus analysis if the bending filter is linear. Another possibility is an adaptive filter in which the gains are self adjusting. Both possibilities are discussed in this report.

An analytical investigation of the concepts was performed using simplified equations. These equations were in agreement with the decoupling principle of the bending filter. From this simplified analysis, relationships between rate-gyro locations, phase and gain requirements of both bending filter and the conventional filter were obtained to determine stability bounds. These relationships were verified by application of the concepts to a representative model booster. Both the linear and adaptive cases were simulated. Stability was achieved for both cases for the nominal vehicle configuration and for 100% increase in bending mode slopes. The adaptive system maintained stability for as much as $\pm 25\%$ variations in first bending mode frequency and $\pm 40\%$ variations in second bending mode frequency.

II. PROBLEM STATEMENT

Large space boosters such as Saturn and Nova are designed to accomplish varied space missions involving large payloads. These vehicles are necessarily long and slender and possess low frequency structural bending modes in the proximity of rigid body control frequencies. State variables, when measured by conventional sensors, are contaminated by the elastic modes which, if reinforced through the control system, cause instability and possible destruction of the vehicle. Conventional gain stabilization, which has been successfully applied to stabilize structural feedback in smaller missiles, is inadequate for the larger vehicles for the following reasons: (1) low frequency bending modes cannot be sufficiently attenuated by low pass filters without severely lagging the control response, and (2) bending mode antinodes change during flight time such that optimum positioning of the gyros for gain stabilization is difficult.

It thus becomes evident that one or more low bending modes must be phase stabilized. Gyro locations for conventional phase stabilization are limited to those positions at which the bending mode slopes are small in order to reduce coupling effects. Furthermore, the locations must be readily accessible. The conventional filter allows little additional phase stability margin since it is constrained in the following ways: it must not destabilize other bending modes or slosh modes, it must not appreciably lag the rigid body signal, and finally, it should be as simple and reliable as possible.

These problems are compounded by inaccurate knowledge of the numerical values of both bending mode slopes and frequencies.

Because of the difficulties in conventional filtering and positioning, a different approach to gain and phase stabilization is considered in this report. This method utilizes two rate gyros at different locations along the vehicle axis. Basically this procedure is to subtract outputs of two rate gyros to obtain a pure "bending" signal; i.e., the rigid body control mode is eliminated from the bending modes. This bending signal is then operated on by a specially designed filter in a manner which will gain stabilize or phase stabilize the elastic modes. This filter, called the bending filter, may be simply a combination of linear band-pass filters, each filter being designed to stabilize a particular bending mode. On the other hand, a more elaborate adaptive bending filter might be considered if needed.

Some preliminary design techniques for the special bending filter are outlined in this report. If the filter is linear, it is amenable to the usual root locus analysis. Design of an adaptive filter is, in general, more difficult. A simple example of an adaptive filter is presented, however, designed on the basis of a quasi-linear preliminary analysis and an analog response study.

III. METHOD OF APPROACH

The fundamental reason for using two rate gyros is to provide a means of decoupling the rigid body and elastic feedback signals. If a single rate gyro is used, unless the location is at a bending antinode, the rate feedback contains both rigid body and elastic components. If, however, the outputs of two identical rate gyros at different locations along the vehicle axis are subtracted, the resultant signal contains pure bending information. This "pure" bending signal may be adjusted or filtered in various ways without any corresponding operation on a rigid body signal. This pure (but not total) bending signal is thus decoupled from the rigid body signal.

In Figure 1 a general block diagram of a dual rate gyro system is presented. The control equation for this system is a conventional linear combination of angle-of-attack, rate gyro, and position gyro feedbacks with an additional adjusted bending signal ϕ_{ba} . ϕ_{ba} is the output of a special bending filter which operates on the pure bending signal $\dot{\phi}_1 - \dot{\phi}_2$.

The primary purpose of the bending filter is to decouple the bending modes from one another. Gyro blending systems without the bending filter cannot produce a stabilizing adjustment on one bending mode without a corresponding adjustment, which is in many cases destabilizing, on other bending modes. The bending filter serves to separate the modes and thus minimizes the interaction between different modes. Each mode can, to an extent, be stabilized independently of the others.

For this reason a preliminary investigation of the system can be considerably simplified by an analysis which treats each mode independently. This "quick look" analysis based on simplified decoupled equations can provide insight as to gain and phase bending filter characteristics required to stabilize a bending mode for particular gyro locations. This analysis is presented in the following section.

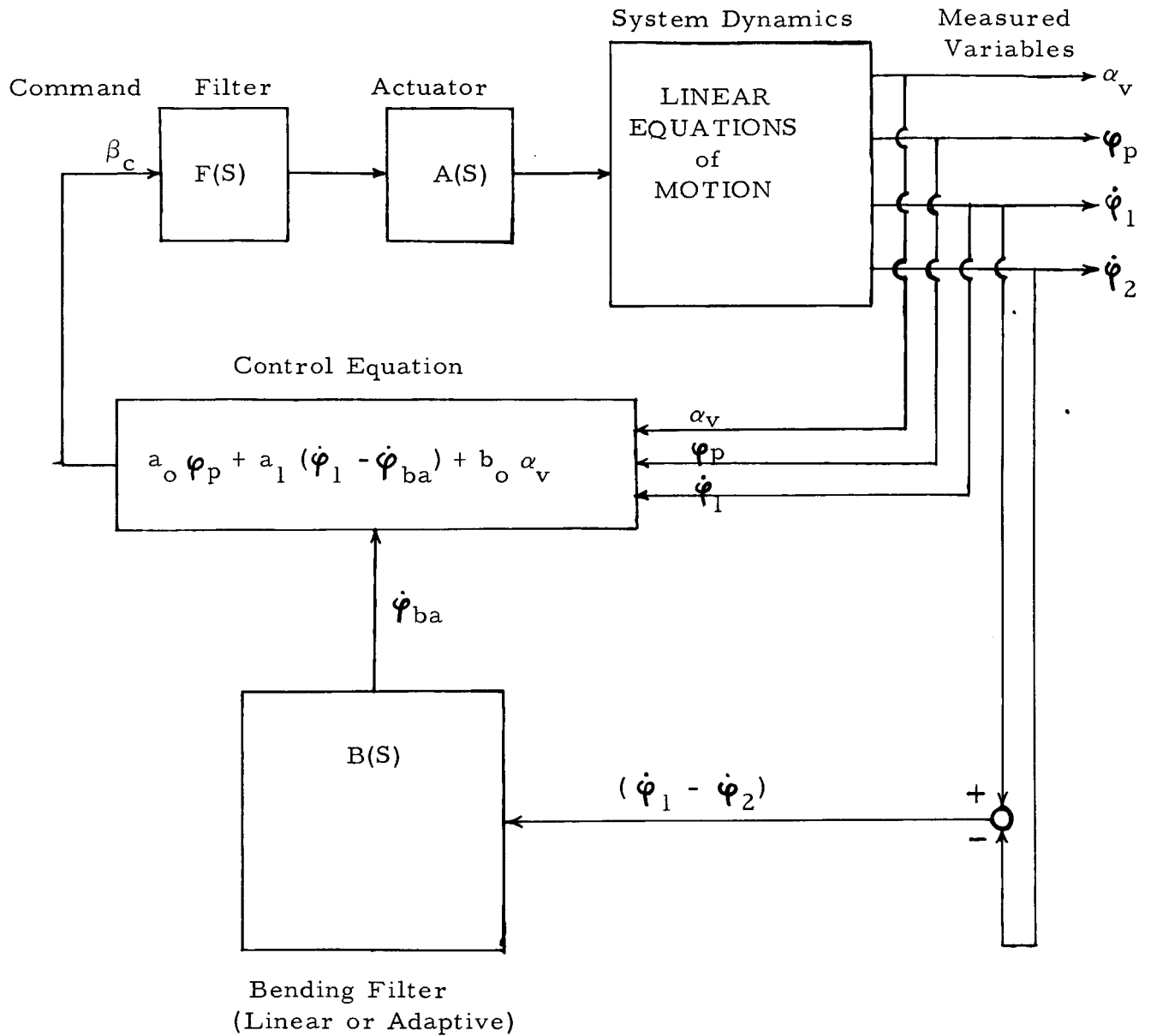


Figure 1. GENERAL BLOCK DIAGRAM OF DUAL GYRO SYSTEM WITH BENDING FILTER

A. Preliminary Design Concept

The following simplified analysis assumes a single general bending mode. In this treatment coupling influences between this bending mode and the rigid body are not considered. Using this 'decoupling' assumption simplified formulas can be developed which approximate the closed loop frequency and damping of the bending mode in a neighborhood of the open loop bending pole. These formulas are quite useful in determining approximate gain and phase requirements of the filters to stabilize the bending mode. Other effects such as stability of filters or interaction between filters and rigid body cannot be determined by this analysis. These effects are seen in a root locus analysis presented in the "results" section of this report. (The decoupled mode analysis is useful, however, in a region near the open loop bending pole and in this region is in agreement with the complete root locus analysis.) For a more detailed discussion on decoupled mode analysis the reader should consult Reference 1.

1. Derivation

Using the notation of the Laplace Transform the following equations can be written:

The control equation is

$$\beta_c(s) = a_o \phi_p(s) + a_1 \left[s\phi_1(s) - s\phi_{ba}(s) \right] + b_o \alpha_v(s) \quad (1)$$

where the sensor outputs are

$$\begin{aligned} \phi_p(s) &= \phi_R(s) - Y_p' \eta(s) \\ s\phi_1(s) &= s\phi_R(s) - Y_1' s\eta(s) \\ s\phi_2(s) &= s\phi_R(s) - Y_2' s\eta(s) \\ \alpha_v(s) &= \alpha_R(s) - Y_v' \eta(s) - \frac{Y_v}{V} s\eta(s) \end{aligned}$$

and the output of the bending filter is

$$S\varphi_{ba}(S) = B(S) \left[S\varphi_1(S) - S\varphi_2(S) \right] = - B(S) (Y_1^I - Y_2^I) S\eta(S)$$

where $B(S)$ is the transfer function of the bending filter.

The engine gimbol angle β is given by

$$\beta(S) = F(S) A(S) \beta_c(S) \quad (2)$$

where $F(S)$ and $A(S)$ denote the respective transfer functions of the conventional filter and actuator.

The bending mode equation is

$$(S^2 + 2\zeta_B \omega_B S + \omega_B^2) \eta(S) = \frac{Y \beta^N}{M_B} \beta(S). \quad (3)$$

Equations (1) can be combined with equation (2) and $\beta(S)$ may then be written as the sum of rigid and elastic components,

$$\beta(S) = \beta_R(S) + \beta_B(S) \quad (4)$$

where

$$\beta_R(S) = F(S) A(S) \left[a_0 \varphi_R(S) + a_1 S \varphi_R(S) + b_0 \alpha_R(S) \right]$$

and

$$\beta_B(S) = - F(S) A(S) \left[A_0 \eta(S) + A_1(S) S \eta(S) \right]$$

where A_0 and $A_1(S)$ are introduced to shorten notation.

$$A_o = a_o Y'_p + b_o Y'_v \quad (5)$$

$$A_1(S) = a_1 \left[Y'_1 - B(S) (Y'_1 - Y'_2) \right] + b_o \frac{Y_v}{V}$$

According to the decoupling assumption $\beta_R(S)$ may be used with a set of rigid body dynamic equations with $\beta_B(S)$ considered as a non-reinforcible disturbance. This constitutes the rigid body control problem. Likewise the flexible body problem can be studied by combining equations (3) and (4) and treating $\beta_R(S)$ as a forcing function. In general, the two problems can be separated whenever the amplitudes of the bending oscillations are small as is the case for low structural gains.

Considering only the flexible body problem, equations (3) and (4) yield the following vibration equation:

$$\left\{ S^2 + \left[2\zeta_B \omega_B + \frac{Y_{\beta N \beta}}{M_B} F(S) A_1(S) \right] S + \left[\omega_B^2 + \frac{Y_{\beta N \beta}}{M_B} A_o F(S) \right] \right\} \eta(S) = \frac{Y_{\beta N \beta}}{M_B} \beta_R(S) \quad (6)$$

Associated with equation (6) is the following characteristic equation:

$$S^2 + \left[2\zeta_B \omega_B + \frac{Y_{\beta N \beta}}{M_B} F(S) A_1(S) \right] S + \left[\omega_B^2 + \frac{Y_{\beta N \beta}}{M_B} A_o F(S) \right] = 0 \quad (7)$$

or

$$S^2 + \left[2\zeta_B \omega_B + \frac{Y_{\beta N \beta}}{M_B} R_F(S) R_A(S) e^{j[\phi_F(S) + \phi_A(S)]} \right] S + \left[\omega_B^2 + \frac{Y_{\beta N \beta}}{M_B} A_o R_F(S) e^{j\phi_F(S)} \right] = 0$$

where

$$F(S) = R_F(S) e^{j\phi_F(S)} = R_F(S) \left[j \sin \phi_F(S) + \cos \phi_F(S) \right] \quad (8)$$

$$A_1(S) = R_A(S) e^{j\phi_A(S)} = R_A(S) \left[j \sin \phi_A(S) + \cos \phi_A(S) \right]$$

and the following relationships exist between $A_1(S)$ and $B(S)$:

$$\begin{aligned} R_A(S) \sin \phi_A(S) &= -a_1(Y_1' - Y_2') R_B(S) \sin \phi_B(S) \\ R_A(S) \cos \phi_A(S) &= a_1 \left[Y_1' - (Y_1' - Y_2') R_B(S) \cos \phi_B(S) \right] + b_0 \frac{Y_v}{V}. \end{aligned} \quad (9)$$

It is known from the decoupling assumption that the characteristic equation (7) is valid for determining a root in the vicinity of the open loop bending pole, where structural feedback is small. If only the root in this region is of interest, equation (7) may be replaced by a second degree equation which contains approximately the same root. This can be accomplished if the region of interest is sufficiently small that the magnitude and phase contribution to equation (7) due to filters and the actuator can be assumed invariant throughout this region. Furthermore $\sigma_B < \omega_B$ in this region, and the substitution $S = j\omega_B$ can be made in the transfer functions of filters and actuator.

Using the above simplification and relations of the form (8) equation (7) becomes:

$$\begin{aligned} S^2 + \left\{ 2\zeta_B \omega_B + \frac{Y_{\beta N\beta}}{M_B} R_F(j\omega_B) \left[\cos(\phi_F(j\omega_B) + \phi_A(j\omega_B)) \sin(\phi_F(j\omega_B) + \right. \right. \\ \left. \left. + \phi_A(j\omega_B)) j \right] \right\} S + \left\{ \omega_B^2 + \frac{Y_{\beta N\beta}}{M_B} A_0 R_F(j\omega) \left[\cos \phi_F(j\omega_B) + \sin \phi_F(j\omega_B) j \right] \right\} = 0. \end{aligned} \quad (10)$$

In order to avoid solving an equation with complex coefficients further use is made of the assumption that in the transfer functions for the actuator and filters, $S \approx j\omega_B$. Thus in the above equation j may be replaced S/ω_B . The following quadratic equation results:

$$S^2 + \left\{ \frac{2\zeta_B \omega_B + \frac{Y_{\beta\beta} N_{\beta\beta}}{M_B} R_F(j\omega_B) \left[R_A(j\omega_B) \cos(\phi_F(j\omega_B) + \phi_A(j\omega_B)) + \frac{A_O \sin \phi_F(j\omega_B)}{\omega_B} \right]}{1 + \frac{Y_{\beta\beta} N_{\beta\beta}}{M_B} \frac{R_F(j\omega_B) R_A(j\omega_B)}{\omega_B} \sin(\phi_F(j\omega_B) + \phi_A(j\omega_B))} \right\} S + \left\{ \frac{\omega_B^2 \frac{Y_{\beta\beta} N_{\beta\beta}}{M_B} A_O R_F(j\omega_B) \cos \phi_F(j\omega_B)}{1 + \frac{Y_{\beta\beta} N_{\beta\beta}}{M_B} \frac{R_F(j\omega_B) R_A(j\omega_B)}{\omega_B} \sin(\phi_F(j\omega_B) + \phi_A(j\omega_B))} \right\} = 0. \quad (11)$$

The roots of this equation are given by $S = \sigma' + j\omega'$ where

$$\sigma' = - \left\{ \frac{\zeta_B \omega_B + \frac{1}{2} \frac{Y_{\beta\beta} N_{\beta\beta}}{M_B} R_F(j\omega_B) \left[R_A(j\omega_B) \cos(\phi_F(j\omega_B) + \phi_A(j\omega_B)) + \frac{A_O \sin \phi_F(j\omega_B)}{\omega_B} \right]}{1 + \frac{Y_{\beta\beta} N_{\beta\beta}}{M_B} \frac{R_F(j\omega_B) R_A(j\omega_B)}{\omega_B} \sin(\phi_F(j\omega_B) + \phi_A(j\omega_B))} \right\} \quad (12)$$

and

$$\omega' = \sqrt{\frac{\omega_B^2 + \frac{Y_{\beta\beta} N_{\beta\beta}}{M_B} A_O R_F(j\omega_B) \cos \phi_F(j\omega_B)}{\frac{Y_{\beta\beta} N_{\beta\beta}}{M_B} \frac{R_F(j\omega_B) R_A(j\omega_B)}{\omega_B} \sin(\phi_F(j\omega_B) + \phi_A(j\omega_B))} - \sigma'^2}. \quad (13)$$

2. Stability Bounds

In order to stabilize the bending mode, the parameters R_F , ϕ_F , ϕ_A and A_O must be chosen such that $\sigma' < 0$. Since the decoupling assumption requires that the denominator of σ' can never be zero the general stability condition of a decoupled bending mode can be stated as follows:

$$N(\phi_F, R_F, \phi_A, R_A) < 0$$

where by definition

$$N = - \left[\zeta_B \omega_B + \frac{1}{2} \frac{Y_B N_B}{M_B} R_F \left(R_A \cos (\phi_F + \phi_A) + \frac{A_O}{\omega_B} \sin \phi_F \right) \right]. \quad (14)$$

If the stability condition can be satisfied by a choice of parameters such that

$$\left| \frac{1}{2} \frac{Y_B N_B}{M_B} R_F \left[R_A \cos (\phi_F + \phi_A) + \frac{A_O}{\omega_B} \sin \phi_F \right] \right| < \zeta_B \omega_B$$

then the bending mode is said to be "gain" stable. If this condition is not satisfied, and $N < 0$ anyway because of a proper choice of the phase ϕ_B and ϕ_F and the sensor positions (which determine the algebraic signs of the slopes Y'_1 , Y'_2 , and Y'_3), the mode is "phase" stable.

If a conventional stabilization system without the bending filter and with only one rate gyro is used then $R_B = 0$ and

$$R_A = a_1 Y'_1 + b_o \frac{Y_v}{V}$$

$$\phi_A = 0^\circ \quad \text{from (9).}$$

This conventional system can gain stabilize only by choosing either R_F small or by finding sensor locations such that Y'_1 and Y'_p are small. Phase stabilization can be accomplished only by proper choice of ϕ_F and the sensor locations. If the dual gyro stabilization system is used, two additional parameters, R_B and ϕ_B , may be used. Thus values of R_A and ϕ_A where $R_A = R_A(R_B, \phi_B)$ and $\phi_A = \phi_A(R_B, \phi_B)$ can be chosen to stabilize the mode regardless of the values of Y'_1 , R_F , and ϕ_F provided the two rate gyros are properly spaced such that $Y'_1 \neq Y'_2$.

In order to establish stability bounds of the bending filter phase ϕ_B and gain R_B , it is advantageous to write N in terms of these quantities. Rewriting N in the following form:

$$N = - \left[\zeta_B \omega_B + \frac{1}{2} \frac{Y_{\beta\beta}^N}{M_B} R_F \left(R_A \cos \phi_A \cos \phi_F - R_A \sin \phi_A \sin \phi_F + \frac{A_o}{\omega_B} \sin \phi_F \right) \right]$$

and substituting from Equation 8: (15)

$$N = - \left\{ \zeta_B \omega_B + \frac{1}{2} \frac{Y_{\beta\beta}^N}{M_B} R_F \cos \phi_F \left[a_1 \left(Y'_1 - (Y'_1 - Y'_2) R_B \cos \phi_B \right) + b_o \frac{Y_v}{V} \right] + \frac{1}{2} \frac{Y_{\beta\beta}^N}{M_B} R_F \sin \phi_F \left[a_1 (Y'_1 - Y'_2) R_B \sin \phi_B + \frac{a_o}{\omega_B} \right] \right\}. \quad (16)$$

Or in another form:

$$N = - \left\{ \zeta_B \omega_B + \frac{1}{2} \frac{Y_{\beta\beta}^N}{M_B} R_F \left[a_1 \left(Y'_1 \cos \phi_F - (Y'_1 - Y'_2) R_B \cos (\phi_F + \phi_B) \right) + \frac{b_o Y_v}{V} \cos \phi_F + \frac{A_o}{\omega_B} \sin \phi_F \right] \right\}. \quad (17)$$

From this equation a lower bound of $|R_B|$ can be determined such that the stability condition $N < 0$ is satisfied. An upper stability bound for R_B exists if the full equations including coupling effects are considered. This upper bound cannot be determined by Equation (17).

The stability condition may be further simplified if the rate gyros are not located near antinodes, that is, Y'_1 or Y'_2 are of the same (or greater) order of magnitude as Y_v , Y'_v , Y'_p , and $\zeta_B \omega_B$. Under this assumption the approximate stability condition is as follows:

$$Y_{\beta} \left[Y'_1 \cos \phi_F - (Y'_1 - Y'_2) R_B \cos (\phi_F + \phi_B) \right] > 0. \quad (18)$$

In this expression Y_β may be either positive or negative, depending on the particular bending mode and on whether or not bending modes are normalized at the nose or tail of the vehicle. If bending is normalized at the nose, $Y_\beta > 0$ for the first mode and $Y_\beta < 0$ for the second. If, however, bending is normalized at the tail $Y_\beta > 0$ for all bending modes.

The inequality (18) determines a stability region in which the boundary is determined from the following equation:

$$\bar{R}_B \cos (\phi_B + \phi_F) = \frac{Y_1'}{Y_1' - Y_2'} \cos \phi_F \quad (19)$$

provided $Y_1' \neq Y_2'$

Equation (19) is quite useful in providing a "quick look" analysis of the type of bending filter needed for various bending modes. It is evident from this equation that if $|Y_1'| > |Y_2'|$, a necessary condition for the stability bound \bar{R}_B to be a minimum is the condition:

$$\phi_B = - \phi_F \quad (20)$$

Of perhaps greater importance is the fact that this is the condition for which the stability bound R_B is least sensitive to changes in ϕ_B . The exact values of the phases ϕ_F and ϕ_B at the bending mode frequencies cannot be known by the filter designer for several reasons. The dynamics of the two rate gyros may not be exactly the same, and the bending mode frequency may not be known with a high degree of accuracy. Thus condition (20) is often a good design criterion since it provides the greatest tolerance for variations in either ϕ_F or ϕ_B . Equation (20) will thus be denoted as the optimum phase condition.

A sketch of Equation (19) is presented in Figure 2-A. An arbitrary ϕ_F is assumed for the sketch. It is further assumed that $|Y_1'| > |Y_2'|$ without loss of generality since the effect of $|Y_1'| > |Y_2'|$ can be seen by replacing ϕ_B by $\phi_B \pm 180^\circ$. It is seen from (18) that for $Y_1' < 0$ the first bending mode is stable for the region $|R_B| > |\bar{R}_B|$. For $Y_1' > 0$ the stability region is $|R_B| < |\bar{R}_B|$. For the second bending mode if bending deflections are normalized at the nose of the vehicle $Y_\beta < 0$ and the stability regions are reversed. If bending deflections are normalized at the tail, however, Y_β has the same sign for all bending modes and stability regions are not reversed.

Note: Bending deflections are assumed normalized at nose for these curves. It is assumed that $|Y'_1| > |Y'_2|$

Figure 2-A

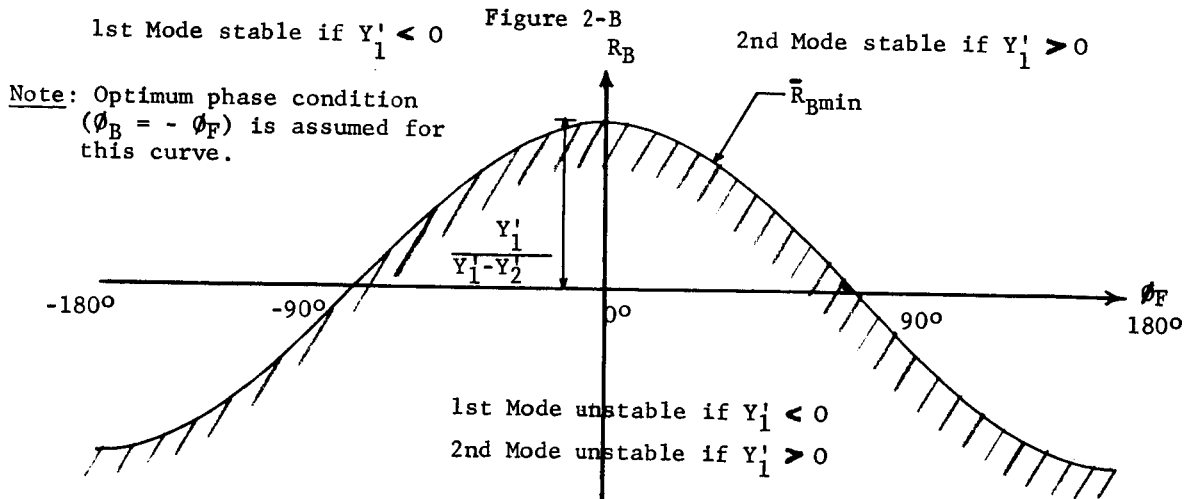
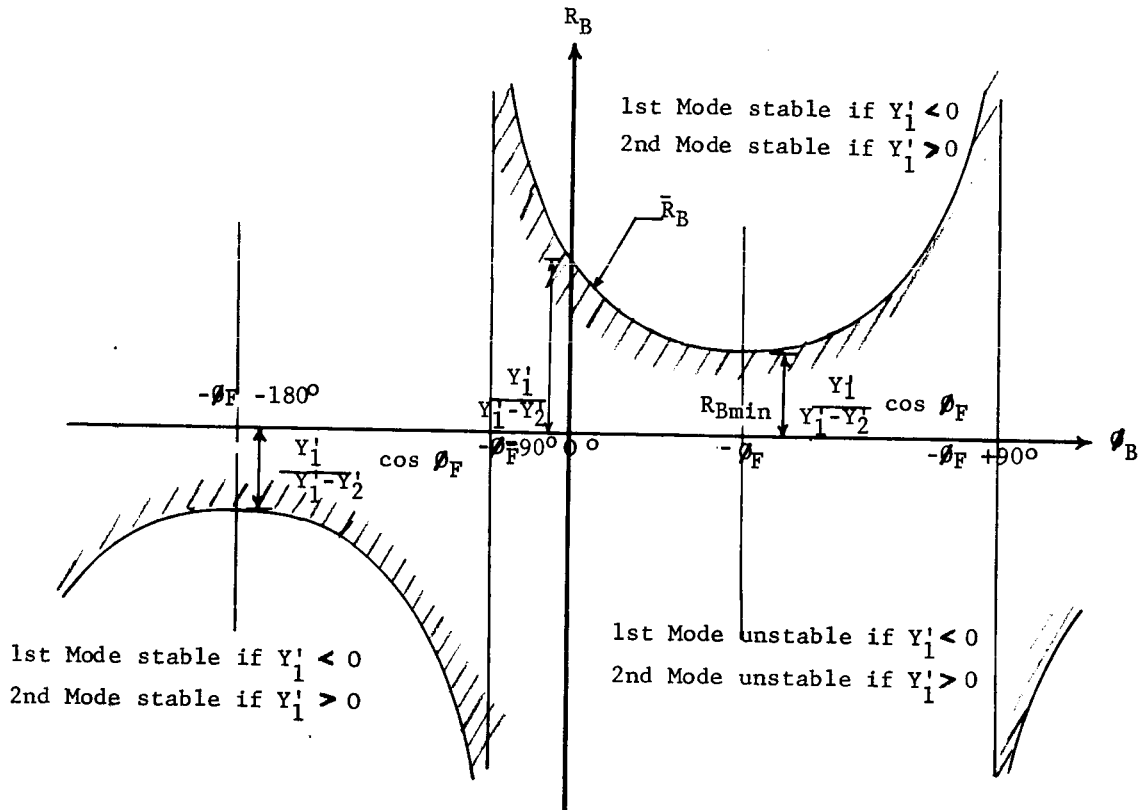


Figure 2: The General Stability Bound Curves

Figure 2-B shows the minimum stability bound (optimum phase condition) as a function of ϕ_F . Stable and unstable regions are indicated. It is easily seen from this figure that for the optimum phase condition and $Y'_1 < 0$ for first mode or $Y'_1 > 0$ for second mode, a choice

of R_B such that $R_B > \frac{Y'_1}{Y'_1 - Y'_2}$ provides stability for all values of ϕ_F .

However, if $Y'_1 > 0$ for the first mode or $Y'_1 < 0$ for the second, stable and unstable regions of Figure 2-B are reversed and R_B must be

chosen such that $R_B < \frac{Y'_1}{Y'_1 - Y'_2}$ in order to stabilize for all ϕ_F . It can

further be shown that even if the optimum phase condition is not satisfied, similar stability bounds independent of ϕ_F can be established provided

$$-\phi_F - 90^\circ < \phi_B < -\phi_F + 90^\circ \quad (21)$$

and

$$Y'_1 - Y'_2 \neq 0.$$

The preceding argument shows an advantage of the bending filter. Since an R_B and ϕ_B can be picked to stabilize a bending mode regardless of R_F and ϕ_F , there is freedom to design the conventional filter to stabilize slosh or other bending modes.

3. Adaptive Stabilization

In order to reduce the amount of a priori knowledge of bending mode data, the bending filter can be made adaptive. This can be done if R_B is self-adjusting such that it automatically seeks values inside the stable regions of Figures 2-A or 2-B. Thus R_B becomes a function of stability. Let $R_B = R_B(\sigma')$ have the following properties: R_B is a bounded function of stability. Initially $R_B = R_o$. If the bending equation is stable, R_B remains constant at the initial value R_o . If the bending equation is unstable R_B increases until a stabilizing value is reached, then levels off at that value.

In order to design a stabilizing system with an adaptive gain R_B with the above properties, three problems are encountered. These problems are as follows:

- 1). How can stability or instability of a bending mode be sensed?

- 2). How can R_0 be selected such that increasing R_B always passes through a stable region?
- 3). Can the nonlinear effect of a changing R_B destabilize?

The first problem is not difficult for a dual gyro system since a pure bending signal can be obtained by subtracting the outputs of the two rate gyros. The rectified output of the bending signal provides stability information. An increasing signal indicates instability; a decreasing or constant signal indicates stability.

In problem two, the choice of R_0 depends on how much adaptivity is needed. Assume, for the first case, it is desired to stabilize without a careful analysis of gyro locations or filter phases. For this case choose R_0 a negative number of sufficiently large magnitude that

$$R_0 < - \left| \frac{Y'_1}{Y'_1 - Y'_2} \right| . \quad \text{It can be seen from Figure 2-A that if } \phi_B \neq -\phi_F \pm 90^\circ,$$

an increasing R_B will intersect the stability bound curve \bar{R}_B , thus always passing through a region of stability. If the region of stability is below the \bar{R}_B curve, R_B (σ') should stop increasing and R_B never intersects \bar{R}_B . Such an adaptive system should stabilize for any gyro positions, with the single restriction that adequate separation exists between the values Y'_1 and Y'_2 .

Assume, in the second case that ϕ_F is between -90° and 90° , and $\phi_B \neq -\phi_F \pm 90^\circ$. Since ϕ_F is known within these limits, it can be seen from Figure 2-B that for $R_0 = 0$, an increasing R_B crosses the \bar{R}_B curve and will pass through a stability region. In this case, as well as in the first case, the single restriction is that Y'_1 and Y'_2 are not approximately equal. Another possible restriction for both cases is that $\phi_B \neq \phi_F \pm 90^\circ$. For this condition the system may be either stable or unstable, depending on the effects of the position gyro and the angle of attack meter.

The third problem includes the following considerations. If the response of R_B is too slow, the bending vibrations may build up to dangerous proportions before a stable region is reached. If, on the other hand, the response is too fast, R_B may overshoot the stability region passing into a region in which the decoupled mode equations are not realistic. Furthermore, the stability bounds of Figure 2-A and 2-B were determined on the basis of linearity of Equation (6). If R_B becomes a function of stability, the linearity assumption is not strictly valid. Finally, a stabilizing function $R_B(\sigma')$ is not unique, and certain type

functions may be more desirable than others. For these reasons, a method of quick analysis of the effects of various R_B functions should be useful. This can be accomplished by analyzing Equation (6) with the equation

$$R_B(\sigma') = F(\dot{\eta}). \quad (22)$$

This is a general adaptivity equation which indicates that $R_B(\sigma')$ is determined by measuring $\dot{\eta}$.

For simplicity assume $\phi_F = 0^\circ$, $R_F = 1$ and the optimum phase condition such that $\phi_B = 0^\circ$. The system to be investigated is:

$$\ddot{\eta} + \left\{ 2\zeta_{BB} \omega_B + \frac{Y_{\beta}^N \beta}{M_B} a_1 \left[Y_1^1 - R_B(Y_1^1 - Y_2^1) \right] \right\} \dot{\eta} + \left(\omega_B^2 + \frac{Y_{\beta}^N \beta}{M_B} A_o \right) \eta = \frac{Y_{\beta}^N \beta}{M_B} \beta_R$$

$$R_B = F(\dot{\eta}). \quad (23)$$

Stability of Equation (23) can very easily be investigated using a small analog computer such as the TR-10. The bending equation can be wired on the computer and several type functions for $F(\dot{\eta})$ can be successively simulated on the computer. Using this method, simplicity of implementation can be used as a criteria, as well as absolute stability.

In order to perform a mathematical investigation of (23) the following general form should be used.

$$\ddot{\eta} + g(\dot{\eta})\dot{\eta} + \omega'^2 \eta = F(t). \quad (24)$$

In this equation $F(t)$ is a forcing function, $g(\dot{\eta})$ a nonlinear damping, and ω' a constant. The general adaptive bending problem depends upon the class of functions $g(\dot{\eta})$ for which Equation (24) is stable.

For certain special functions $g(\dot{\eta})$, an analytic solution to Equation (24) may be found. An approximate solution may be found by setting $g(\dot{\eta}) = \mu h(\dot{\eta}) h(\dot{\eta})$ where $\mu \ll 1$, and taking a variational equation about $\phi(t)$, where $\phi(t)$ is a solution of the linear equation:

$$\ddot{\eta} + \omega'^2 \eta = F(t).$$

For a treatment on this method, see Reference 2 or 3.

B. Application of the Concepts

1. Stabilization Philosophy

In order to apply the concepts previously discussed to a particular booster some stabilization philosophy must be adopted. For application to a representative C-I booster, the following stabilization philosophy was used: A conventional low pass filter is used to gain stabilize the third and higher bending modes. The bending filter, which may be either linear or adaptive, is used only to stabilize the first and second bending modes.

A block diagram of the bending filter is presented in Figure 3. The bending filter consists of two band-pass filters, B_1 and B_2 , in parallel and tuned to the first and second bending modes, respectively, such that the sum of the weighted outputs of the two filters is ϕ_{ba} . A Bode plot and transfer function of one of the band pass filters is presented in Figure 4. It should be pointed out that this band-pass filter is not unique. For stabilizing the first bending mode, a low-pass filter might be acceptable. Furthermore, an RLC band-pass filter might perform better than the RC filter. The RC filter was used as a basis for study because it is easily realizable, and the phase changes less with respect to frequency.

One way to increase the adaptivity of the system is to use tracking filters for B_1 and B_2 . Such an arrangement, however, may be unnecessary. Computer studies presented in the next section indicate that variations in ω_1 and ω_2 can be tolerated for filters of the form of Figure 3. Simple time programming of filter parameters may be sufficient. For a discussion on tracking filters see Reference 4.

Another way of making the system adaptive has already been discussed in the simplified analysis. K_1 and K_2 adjust automatically to stabilize the first two bending modes. Assume that for $K_1 = 0$ and $K_2 = 0$, the sensors are located such that at least one bending mode is unstable. If, for example, the second mode is unstable, K_2 should automatically increase from zero to some positive stabilizing value, and level off at that value, stabilizing the bending mode.

The problem that remains is to implement the concept electronically.

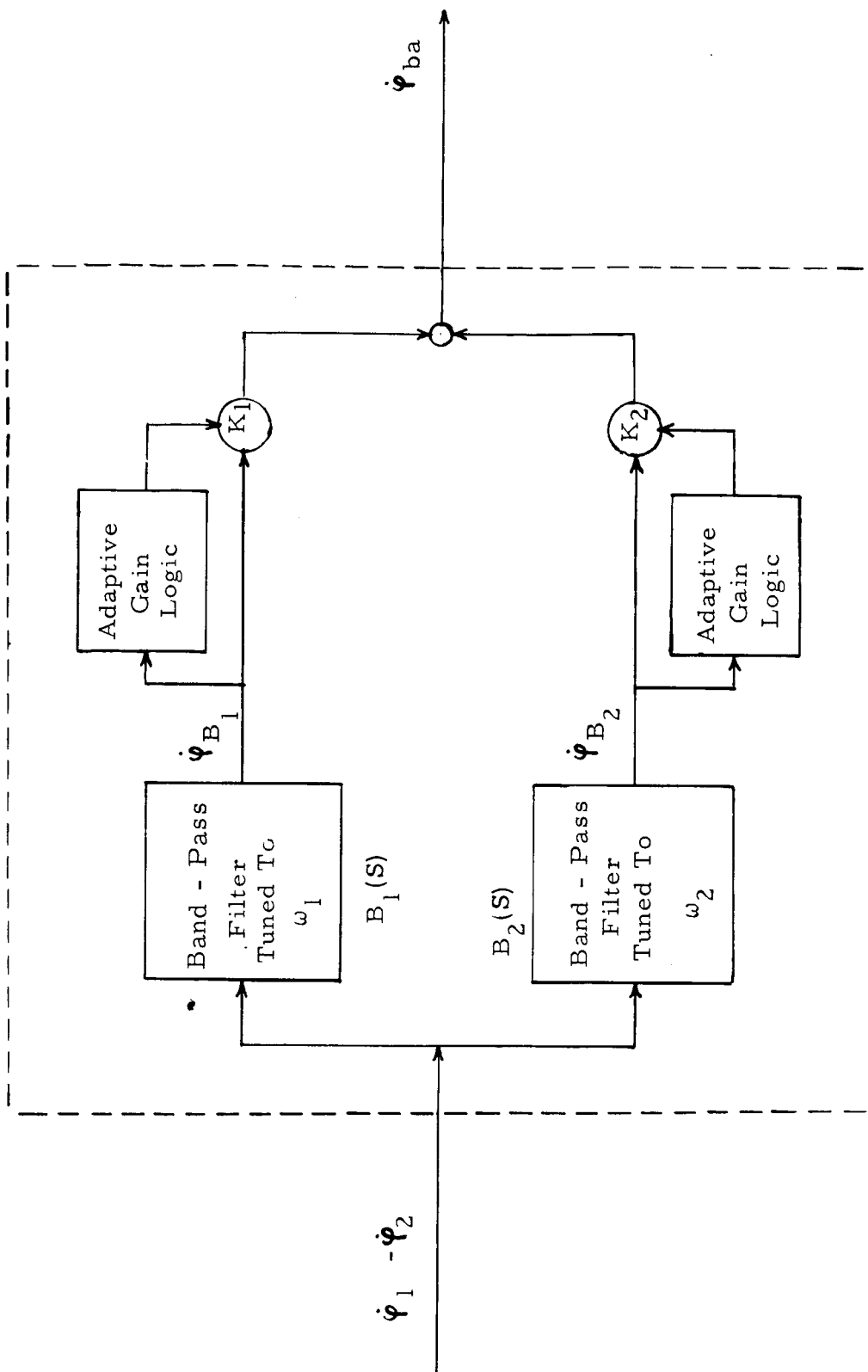


Figure 3. BLOCK DIAGRAM OF BENDING FILTER

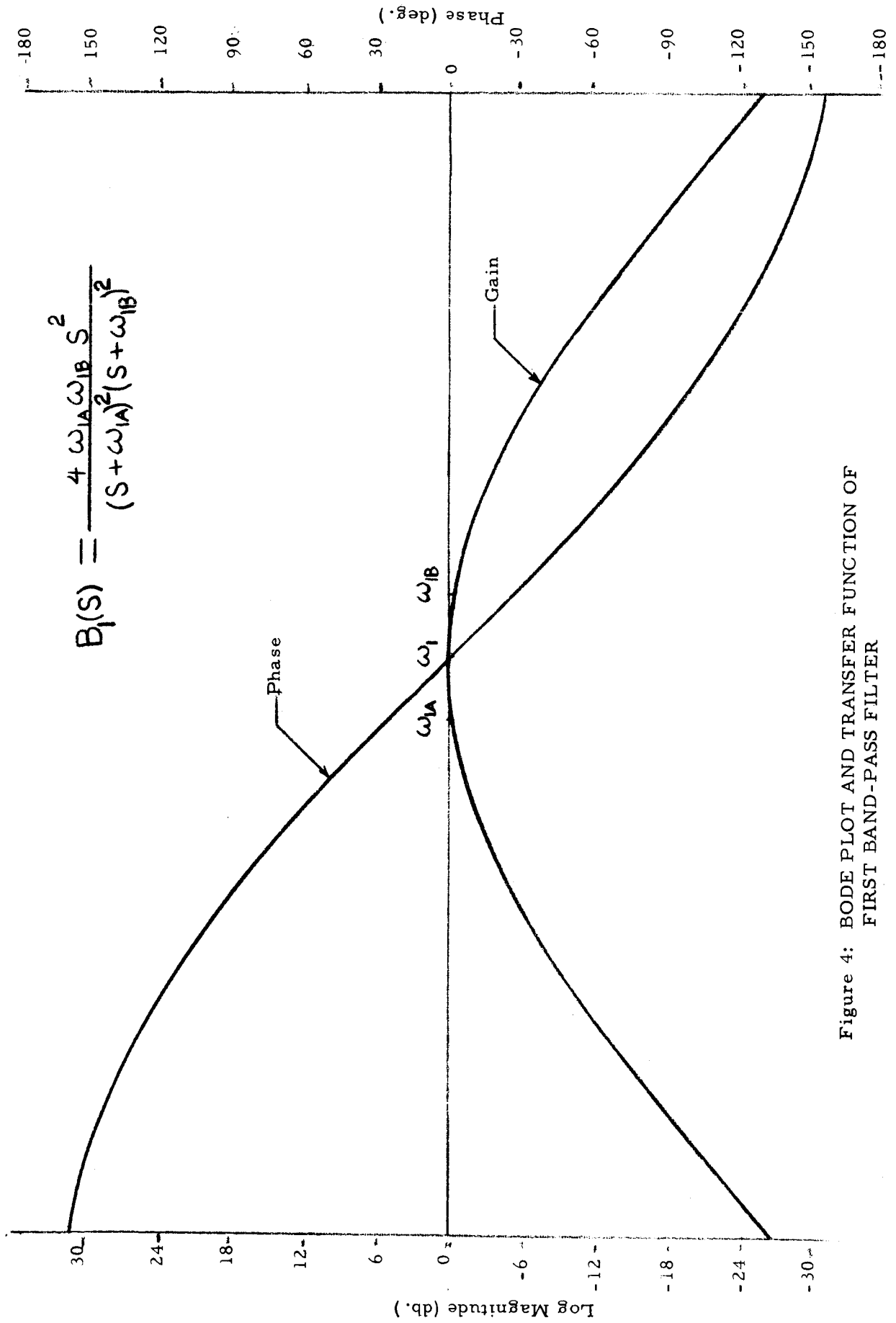


Figure 4: BODE PLOT AND TRANSFER FUNCTION OF FIRST BAND-PASS FILTER

This involves determining some means of sensing stability when the gain has increased to the proper level, then retarding the gain such that it does not continue to increase beyond the stability region. Although many possible schemes can accomplish this, the adaptive gain logic of Figure 5 is perhaps the simplest mechanization. It consists of a full wave rectifier, first order smoothing filter and a multiplier.

The function of the adaptive gain logic of Figure 5 is to produce a gain K_1 , (or K_2) which is proportional to the magnitude of the first (or second) bending mode; thus an increase in bending causes a proportionate gain increase which tends to stabilize. It is seen, however, that a decrease in bending causes a decreasing gain which tends to destabilize. The resultant effect is that K_1 or K_2 settles to a value which produces a stable limit cycle in the bending signal. According to Figure 2-A of the simplified analysis, this corresponds to R_B located on the stability bound curve R_B . According to a root locus interpretation, this corresponds to a gain K_2 such that the second mode operating point is on the $j\omega$ axis.

Although a limit cycle is often undesirable, it is found that by adjusting the parameters, κ and τ , of the adaptive gain logic, the magnitude of the limit cycle can be made extremely small. A quick way of determining the effects of κ and τ on the limit cycle is to program the logic of Figure 12 as Equation (22) of a simplified analysis with Equation (23) on a small analog computer.

2. Basic Equations

Bending stabilization techniques using the linear bending filter and also the adaptive bending filter were investigated. The basic equations which were used for the two studies are listed as follows:

1). Rigid Body

$$\ddot{Z} = \left(\frac{N_\alpha}{m}\right) \alpha_R + \left(\frac{F-X}{m}\right) \phi_R + \frac{(N_\beta)\beta}{m}$$

$$\ddot{\phi}_R + C_1 \alpha_R + C_2 \beta = 0$$

$$\alpha_R = \phi_R + \alpha_W - \dot{Z}/V$$

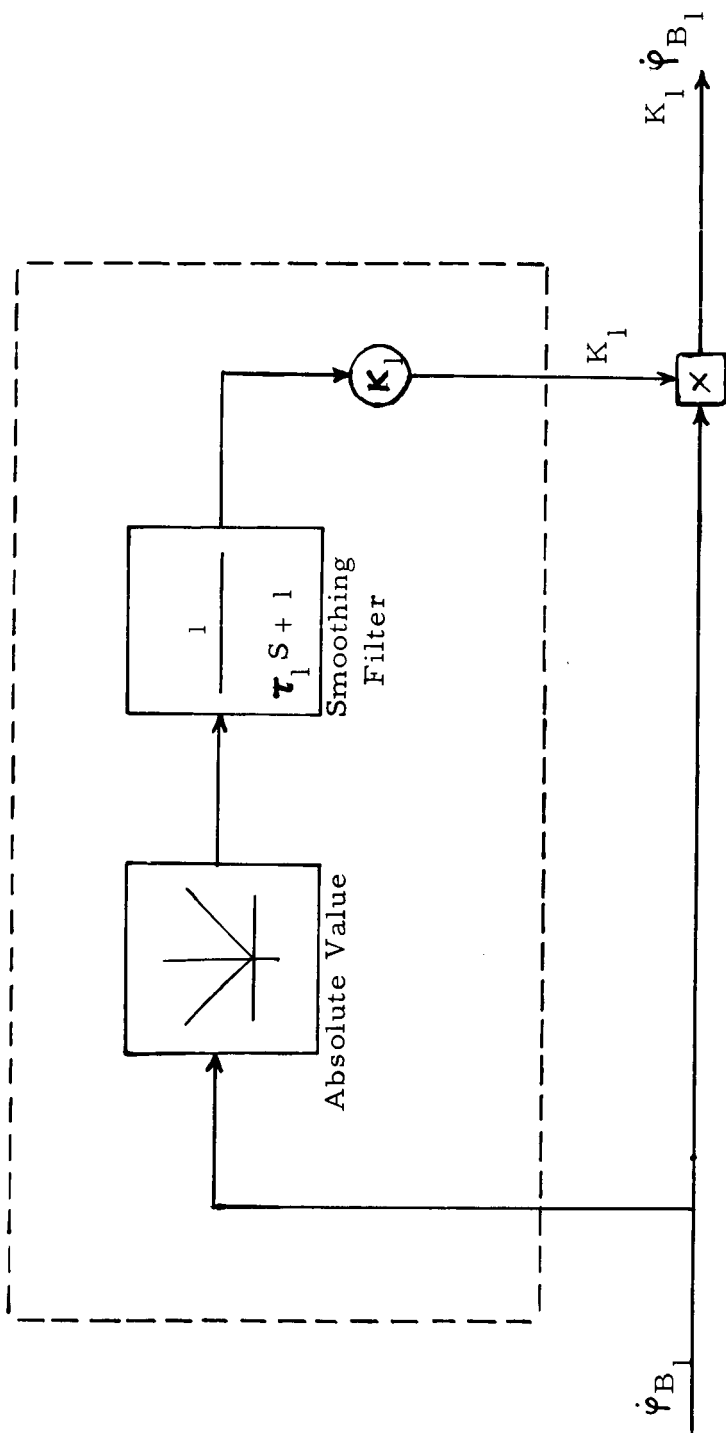


Figure 5. A REPRESENTATIVE ADAPTIVE GAIN LOGIC

2). Elastic Bending

$$\ddot{\eta}_n + 2\zeta_{Bn} \omega_{Bn} \dot{\eta}_n + \omega_{Bn}^2 \eta_n = \frac{Y_{Bn} N_{Bn}}{M_{Bn}} \beta \quad n = 1, 2, 3$$

3). Sensor Outputs

$$\alpha_v = \alpha_R - \sum_{n=1}^3 Y'_{vn} - \sum_{n=1}^3 \frac{Y_v n}{V} \dot{\eta}_n$$

$$\phi_p = \phi_R - \sum_{n=1}^3 Y'_{pn} \eta_n$$

$$\phi_1 = \phi_R - \sum_{n=1}^3 Y'_{1n} \dot{\eta}_n$$

$$\phi_2 = \phi_R - \sum_{n=1}^3 Y'_{2n} \dot{\eta}_n$$

4). Filter and Actuator

$$\beta = F(S) A(S) \beta_c$$

$$A() = \frac{1}{M_2 S^2 + M_1 S + 1}$$

$$F(s) = \frac{K_F}{\left(\frac{S}{\omega_F}\right)^2 + \frac{2\zeta_F}{\omega_F} S + 1}$$

5). Control and Bending Filter Equations

$$\beta_c = a_o \phi_p + a_1(\phi_1 - \phi_{ba}) + b_o \alpha_v$$

$$\dot{\phi}_{ba} = K_1 \phi_{B1} + K_2 \phi_{B2}$$

$$\phi_{B1} = B_1(S) (\phi_1 - \phi_2)$$

$$\phi_{B2} = B_2(S) (\phi_1 - \phi_2)$$

$$B_1(S) = \frac{4\omega_{1A}\omega_{1B}S^2}{(S + \omega_{1A})^2 (S + \omega_{1B})^2}$$

$$B_2(S) = \frac{4\omega_{2A}\omega_{2B}S^2}{(S + \omega_{2A})^2 (S + \omega_{2B})^2}$$

$$\left. \begin{array}{l} K_1 = K_1(t) \\ K_2 = K_2(t) \end{array} \right\} \begin{array}{c} \text{for the linear system} \\ \text{or} \end{array} \left. \begin{array}{l} K_1 = K_1(\phi_{B2}) \\ K_2 = K_2(\phi_{B2}) \end{array} \right\} \begin{array}{c} \text{for the adaptive} \\ \text{system} \end{array}$$

where

$$K_1(\phi_{B1}) = \frac{K_1}{\tau_1 S + 1} |\phi_{B1}|$$

and

$$K_2(\phi_{B2}) = \frac{K_2}{\tau_2 S + 1} |\phi_{B2}|$$

These equations were used to determine a characteristic equation for the linear system from which root locus data was obtained by solving for roots of this equation by a large digital computer. The equations were also programmed for time response studies on an analog computer for both the linear and adaptive systems. For both systems β and β saturation effects of $\pm 7^\circ$ and $\pm 15^\circ/\text{sec}$, respectively, were included. The results of these studies are presented in the following section.

IV. RESULTS

A. The Linear System

The preceding basic equations were used with obsolete Saturn C-1 data. The coefficients were assumed fixed with values corresponding to time of maximum dynamic pressure. The first and second rate gyros were assumed located at stations 1400 and 600 respectively. These locations were chosen in agreement with the condition, as seen from the simplified analysis, that Y_1' is not approximately equal to Y_2' for either first or second bending modes. The position gyro location was assumed at the G&C compartment at station 1500. As seen from the basic equations,

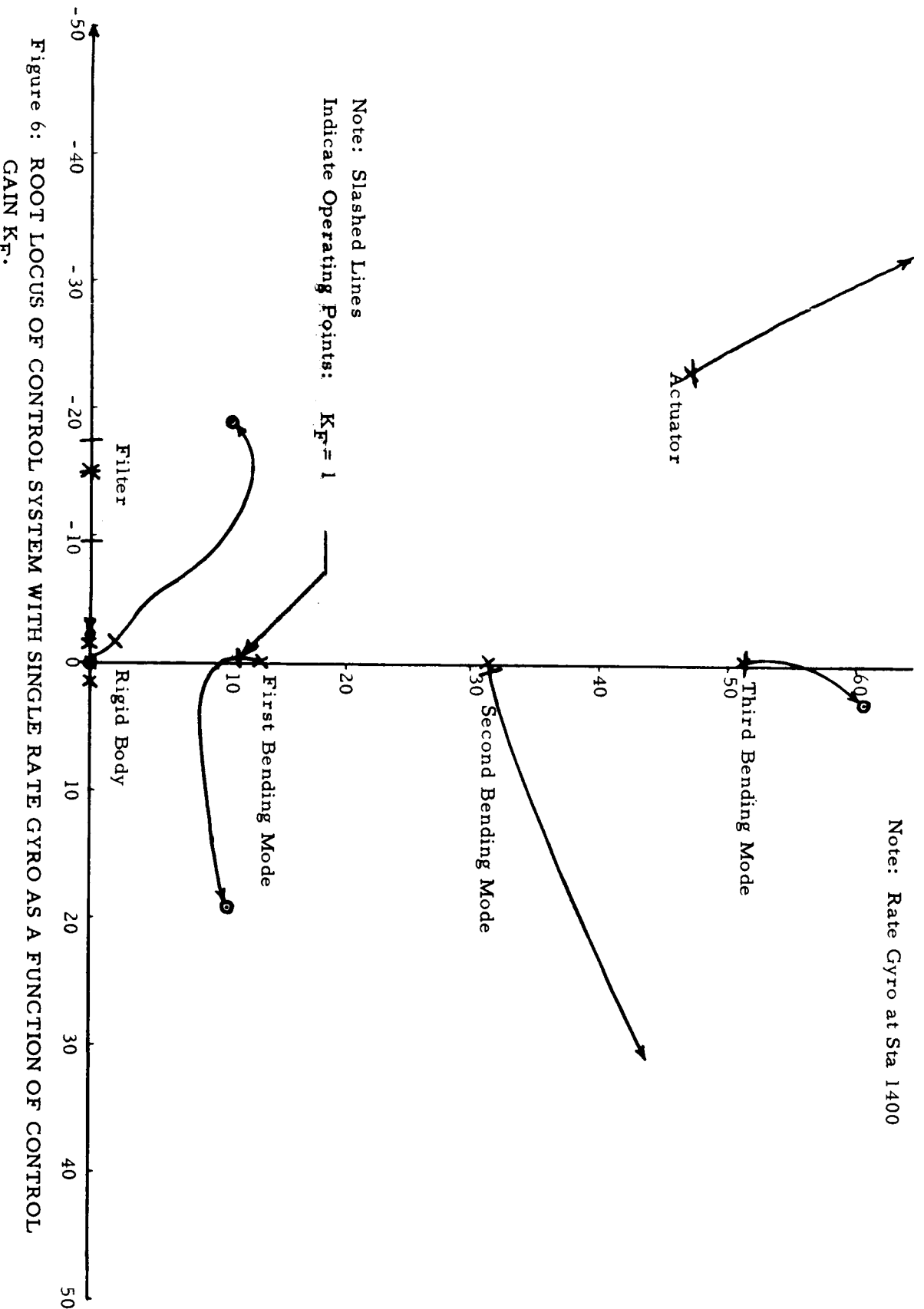
a second order RC network was assumed as a conventional filter for the feedback signal β_c . The break point chosen was $\omega_F = 15$, sufficiently low to gain stabilize the third bending mode, but not the first and second modes. Nominal values for break points in the bending filters are as follows:

$$\omega_{1A} = 9 \quad \omega_{1B} = 16$$

$$\omega_{2A} = 25 \quad \omega_{2B} = 40$$

The effect of the dual gyro system with bending filter can be seen from a comparison of Figures 6 and 7. Figure 6 is a root locus diagram of a conventional system with a single rate gyro located at station 1400 whereas Figure 7 is a root locus diagram of the dual gyro system with the other rate gyro at station 600. The filter gain K_F is the parameter with which the roots vary, all other parameters being fixed. The nominal operating point $K_F = 1$ corresponds to those points at which the traces are slashed by short line segments. It can be seen from Figure 6 that the operating point for the conventional system is unstable for the second bending mode and marginally phase stable for the first bending mode. In Figure 7 this situation is corrected by selecting bending filter gains of $K_1 = .5$ and $K_2 = 1$ to be used with the dual gyro system. In this system the second mode is gain stable and the first mode is phase stable with much larger phase and gain margins. The most critical points in the system are now the third bending mode and filter operating points, both of which have gain margins of 1.8.

The parameters used in Figure 7 are considered nominal, but other values may be used as well. A list of the effects of variations in these parameters upon the operating points of the most critical modes of the system is presented in the following table. In this table two extremes are assumed for each selective parameter of the system and the corresponding frequency and damping of critical modes tabulated. In determining the effect of each off-nominal parameter, the other parameters were fixed at nominal values.



Note: Rate Gyros at Sta 1400 and 600
 First Band-Pass Filter Gain,
 $K_1 = .5$ Second Band-Pass
 Filter Gain, $K_2 = 1$

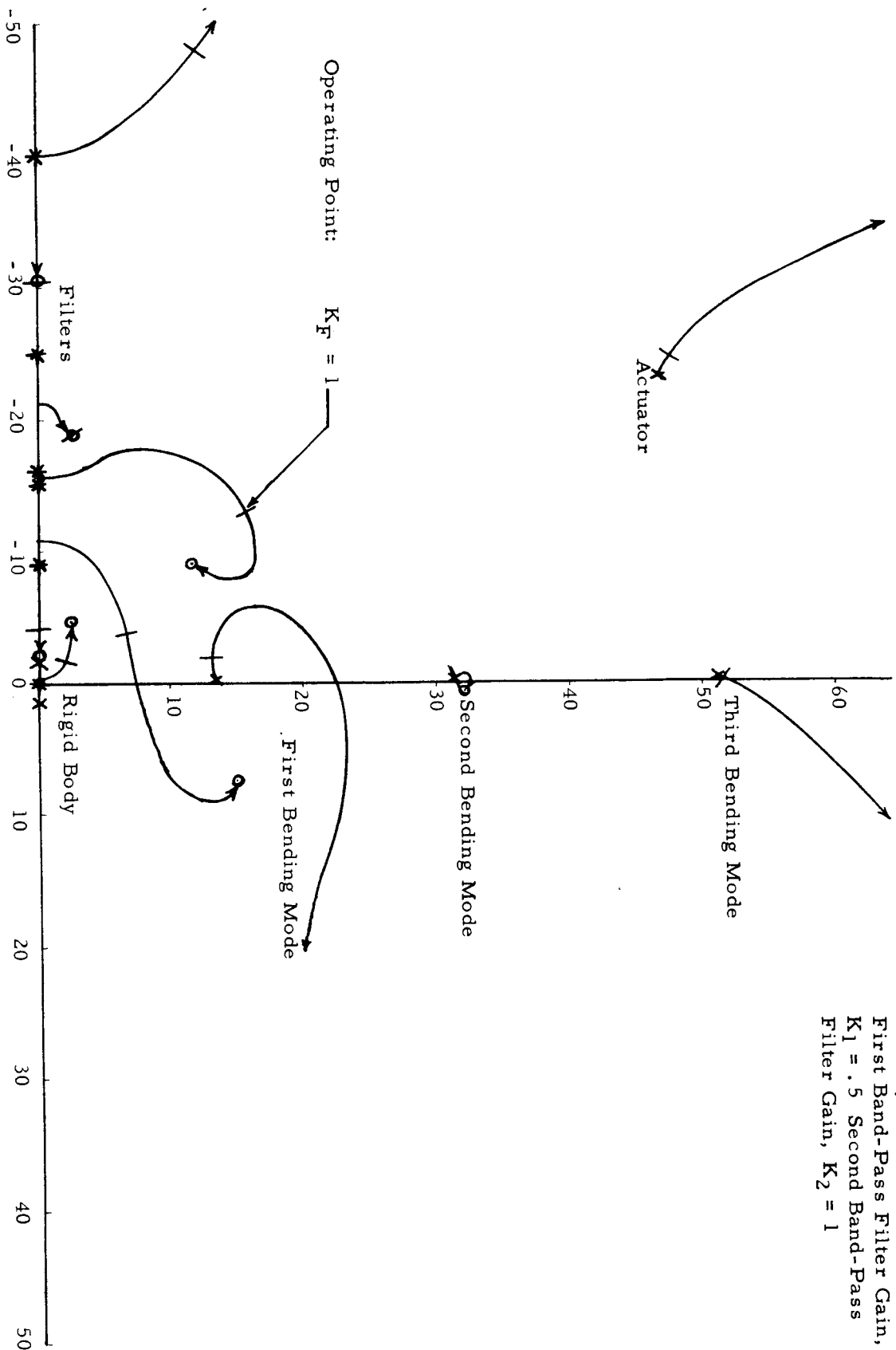


Figure 7: ROOT LOCUS OF CONTROL SYSTEM WITH DUAL RATE GYROS AND BENDING FILTER AS A
 FUNCTION OF CONTROL GAIN K_F .

TABLE I
EFFECT OF SELECTIVE PARAMETERS ON CERTAIN CRITICAL MODES

Lower and Upper Values of Selective Gains	Rigid Body	Filter	First Bending Mode	Second Bending Mode	Third Bending Mode
$K_f = 1.0$	$\omega = 1.93 \sigma = -1.67$	$\omega = 6.68 \sigma = -3.60$	$\omega = 13.13 \sigma = -1.96$	$\omega = 31.46 \sigma = -.25$	$\omega = 51.55 \sigma = -.10$
$K_f = 1.8$	$\omega = 2.2 \sigma = -2.5$	$\omega = 7.4 \sigma = 0$	$\omega = 14.3 \sigma = -4.7$	$\omega = 31.5 \sigma = -.30$	$\omega = 51.8 \sigma = -.0$
$\omega_f = 12$	$\omega = 2.2 \sigma = -1.6$	$\omega = 5.2 \sigma = -3.5$	$\omega = 13.3 \sigma = -.8$	$\omega = 31.45 \sigma = -.2$	$\omega = 51.3 \sigma = -.18$
$\omega_f = 15$	$\omega = 1.93 \sigma = -1.67$	$\omega = 6.68 \sigma = -3.6$	$\omega = 13.13 \sigma = -1.96$	$\omega = 31.46 \sigma = -.25$	$\omega = 51.55 \sigma = -.1$
$K_1 = 0$	$\omega = 1.93 \sigma = -1.67$	$\omega = 0 \sigma = -6.4$	$\omega = 10.7 \sigma = -1.3$	$\omega = 31.29 \sigma = -.24$	$\omega = 51.55 \sigma = -.15$
$K_1 = 1.5$	$\omega = 1.86 \sigma = -1.625$	$\omega = 5.87 \sigma = -1.74$	$\omega = 14.98 \sigma = -.054$	$\omega = 31.77 \sigma = -.24$	$\omega = 51.5 \sigma = -.02$
$K_2 = .65$	$\omega = 1.97 \sigma = -1.7$	$\omega = 6.7 \sigma = -3.6$	$\omega = 13.1 \sigma = -1.96$	$\omega = 31.4 \sigma = 0$	$\omega = 51.6 \sigma = -.10$
$K_2 = 1.75$	$\omega = 1.92 \sigma = -1.67$	$\omega = 7.32 \sigma = -3.45$	$\omega = 12.4 \sigma = -5.26$	$\omega = 31.48 \sigma = -.85$	$\omega = 51.8 \sigma = -.004$
$\omega_{1A} = 6$	$\omega = 1.89 \sigma = -1.68$	$\omega = 5.18 \sigma = -3.61$	$\omega = 12.4 \sigma = -1.45$	$\omega = 31.41 \sigma = -.226$	$\omega = 51.5 \sigma = -.117$
$\omega_{1A} = 16$	$\omega = 1.95 \sigma = -1.68$	$\omega = 8.65 \sigma = -2.88$	$\omega = 14.79 \sigma = -3.38$	$\omega = 31.54 \sigma = -.341$	$\omega = 51.57 \sigma = -.072$
$\omega_{1B} = 9$	$\omega = 1.88 \sigma = -1.66$	$\omega = 5.21 \sigma = -2.91$	$\omega = 12.47 \sigma = -.992$	$\omega = 31.40 \sigma = -.204$	$\omega = 51.55 \sigma = -.122$
$\omega_{1B} = 25$	$\omega = 1.95 \sigma = -1.68$	$\omega = 8.65 \sigma = -4.19$	$\omega = 13.25 \sigma = -3.83$	$\omega = 31.48 \sigma = -.327$	$\omega = 51.57 \sigma = -.085$
$\omega_{2A} = 21$	$\omega = 1.93 \sigma = -1.67$	$\omega = 6.81 \sigma = -3.47$	$\omega = 13.65 \sigma = -2.05$	$\omega = 31.58 \sigma = -.21$	$\omega = 51.5 \sigma = -.076$
$\omega_{2A} = 29$	$\omega = 1.93 \sigma = -1.67$	$\omega = 6.58 \sigma = -3.65$	$\omega = 12.86 \sigma = -1.74$	$\omega = 31.35 \sigma = -.24$	$\omega = 51.6 \sigma = -.14$
$\omega_{2B} = 35$	$\omega = 1.93 \sigma = -1.67$	$\omega = 6.79 \sigma = -3.54$	$\omega = 13.45 \sigma = -2.21$	$\omega = 31.6 \sigma = -.27$	$\omega = 51.5 \sigma = -.066$
$\omega_{2B} = 50$	$\omega = 1.93 \sigma = -1.67$	$\omega = 6.54 \sigma = -3.64$	$\omega = 12.88 \sigma = -1.56$	$\omega = 31.3 \sigma = -.16$	$\omega = 51.6 \sigma = -.18$

It is significant from this table that the parameters in the bending filter cause no appreciable change upon the rigid body operating point, which is approximately the same value as for the conventional single gyro system. It is further seen that for the nominal vehicle, K_1 can range between 0 and 1.5, K_2 between .65 and 1.75 and the system remains stable. Wide variations in ω_{1A} , ω_{1B} , ω_{2A} , and ω_{2B} can also be tolerated. If the conventional filter break point is reduced to 12 the phase lag effect on the rigid body can be seen from the increase in the rigid body operating frequency. Raising ω_F above 15, however, has the effect of decreasing the third mode gain margin. Break points in the bending filter also affect the third mode, but apparently can be lowered below 6 before coupling effects begin to reduce rigid body performance.

Using the nominal values of the selective gains, as determined from the preceding root locus analysis, an analog response study was conducted. The response of a nominal vehicle model with three bending modes is shown in Figure 8. The disturbance α^w which is plotted in Figure 8 is assumed the same for all other analog plots in the study. All three bending modes of the nominal dual rate gyro system of Figure 8 are stable for this disturbance.

In order to provide for inaccuracies in estimates of bending mode slopes and frequencies, analog runs were made for off-nominal values of these parameters using the same selective gains as in Figure 8. For the condition shown in Figure 9A, the first and second bending mode slopes were increased by a factor of 2 at both rate gyro locations. Stability was achieved for this condition. If the third mode slope is also doubled, that mode is no longer gain stable since the bending filter was designed to stabilize only the first two modes. If the conventional filter break point is lowered to provide more attenuation at higher frequencies, all three modes are stable. Such a condition is presented in Figure 9B with $\omega_F = 12$.

Figure 10 depicts the response for off-nominal values of first and second bending mode frequencies. In Figure 10A the first and second modes are decreased by 10% and 15% respectively. In Figure 10B these frequencies are increased by the same percentages. Further analog runs demonstrated that the frequencies may be increased much further than the indicated 10% and 15%, but the negative 15% deviation in second bending mode establishes a stability bound for decreasing ω_{B2} . If a greater tolerance than $\pm 15\%$ ω_{B2} is required, it may be possible to

find other values of the selective gains than nominal, or other gyro locations than were chosen for this study. Still another possibility consists of making the bending filter adaptive.

B. The Adaptive System

It has been previously stated that a bending mode might be stabilized adaptively by increasing a bending filter gain until stability of the mode is sensed. The "increasing gain" stabilizing effect can be seen from root locus plots. Figure 11 presents a locus of "zeros" (points for which $K_F = \infty$) as K_2 increases and $K_1 = 0$. It can be seen from this figure that a zero established by the second mode band-pass filter passes through a proximity of the second bending mode pole as the gain K_2 is increased. For the region of K_2 in which the filter zero is very near the bending mode pole, the mode is gain stable. This is illustrated in Figure 12. It is seen from this sketch that for the zero near the bending pole, the locus from the filter poles does not flow into the zero, but is replaced by the bending mode locus which flows into the zero. It is seen from the sketch that for some values of K_2 , the entire second mode locus is in the left half plane, and that the operating point is sufficiently near the bending pole to be gain stable.

In order for K_1 and K_2 to increase to stabilizing values the adaptive gain logic of Figure 5 is used. Analog response studies using the basic equations for the adaptive system were conducted. For these studies both K_1 and K_2 were given the initial value zero and then they automatically adjusted to positive stabilizing values. These response studies are thought to be conservative since sudden large adjustments in K_1 or K_2 are not so likely during an actual booster flight as continual small adjustments in these parameters over long time intervals.

For the initial condition $K_{10} = K_{20} = 0$ and for the same wind input as in the previous linear study, responses were obtained for a range of values of κ/τ and τ . This study was performed to determine the effects of κ/τ and τ on three critical parameters: the bending limit cycle magnitude L_η , maximum peak-to-peak bending amplitude P_η , and the overshoot ratio M of the adaptive gain, for both first and second bending modes. Data obtained from these response studies was used to plot the curves in Figures 13 through 17.

Examination of the curves in Figures 13 through 17 reveals the following characteristics: For the second mode small values of τ and κ/τ cause large limit cycle magnitudes and peak bending oscillations. As τ and κ/τ increase, both P_η and L_η approach small constant values. It is observed that no limit cycle exists for the first bending mode, the reason being that the first mode is slightly phase stable for $K_1 = 0$. It

is seen that M increases with both κ/τ and τ for both modes. It is important that M not be excessively large. A large value of M_1 or M_2 can mean that the peak value of K_1 or K_2 is near the upper stability bound. For this reason κ/τ and τ should be small. If the requirements, $M < 1.0$ and $L < .1$, are acceptable, a wide range of κ/τ and τ can be found. The values used for the following study are $\frac{\kappa}{\tau} = 8$ and $\tau = 5$ for both bending modes.

Figure 18 presents a response of the adaptive stabilization system. It can be seen that as the second mode bending oscillations increase in magnitude, K_2 increases, stabilizing the bending and reaching a peak value just less than 1. Then as K_2 approaches a steady state value of .65, the bending settles to a small limit cycle. As seen from the figure, the effects of the bending oscillations on α_R , ϕ_R , and β is almost imperceptible. For this case $M_1 = .66$, $M_2 = .50$, $P_{\eta 1} = .13$, $P_{\eta 2} = .12$, $L_{\eta 1} = 0$, and $L_{\eta 2} = .04$.

Off nominal conditions are presented in Figures 19 through 22. Figure 19 shows the response when first and second mode slopes are doubled. For this case K_1 peaks above 1, but stability is maintained. In Figure 20 ω_F is lowered to 12 to stabilize the off-nominal third mode. All three mode slopes are doubled for this case. Figures 21 and 22 show the wide range of ω_{B1} and ω_{B2} which can be tolerated using the adaptive system. Stability can be maintained for $\pm 25\%$ variations in ω_{B1} and $\pm 40\%$ variations in ω_{B2} .

V. CONCLUSION

The purpose of this study was to investigate a dual gyro system with bending filter and to perform a preliminary feasibility analysis of this concept on a representative elastic booster. Simplified equations were used to establish stability bounds and basic trends. These trends were verified by root locus and response studies using the basic equations and approximate Saturn C-I data. Stability was achieved for the representative configuration and using certain off-nominal elastic body parameters for rate gyro locations at stations 1400 and 600.

It should be pointed out that no attempt was made either to optimize gyro locations or bending filter parameters in this study but rather to illustrate the concepts. Better results may be obtained by a modification of the techniques. The method of adaptation, for example, might be improved by choice of an entirely different adaptive gain logic.

Furthermore, it is not known whether or not larger vehicles such as Saturn C-5 or Nova can be stabilized with the same philosophy as

presented here. If difficulty is encountered, it may be possible to redesign the bending filter using a low-pass filter instead of a band-pass filter for first mode stabilization. A more practical philosophy might be to use two band-pass filters to stabilize the second and third bending modes and phase stabilize the first by judicious sensor locations. Other combinations are possible; the best approach depends on the particular problems encountered by specific low bending frequency elastic boosters.

In summary, the results of this study indicate the following possible advantages for using dual rate gyros and bending filter:

- 1). Coupling effects between elastic and rigid body modes as well as between separate elastic modes can be reduced by adjustment of bending filter gains. Since the modes can be treated independently of one another, insight can be obtained by a simplified analysis.
- 2). Since the gains of the bending filter can be chosen to stabilize the low bending modes, more freedom is allowed to design the conventional filter from the standpoint of slosh considerations and other bending modes. A simpler conventional filter can be designed.
- 3). Since the bending filter operates on a pure bending signal, it does not produce phase lag of the rigid body response.

REFERENCES

1. Ryan, R. S., "Stability Considerations of a Space Vehicle in Bending Oscillations for Various Control Sensors," MTP-AERO-62-64 (to be published).
2. Minorsky, Nicholas, "Introduction to Non-linear Mechanics," Ann Arbor, Michigan, Edwards Brothers, Inc., 1947.
3. Andronow, A. A. and Chaikin, C. E., "Theory of Oscillations," Princeton, New Jersey, Princeton University Press, 1949.
4. Davis, B. G., "Frequency Sensors and Variable Notch Filters for Stabilization of Elastic Vibrations in Space Boosters," M-AERO-IN (to be published).

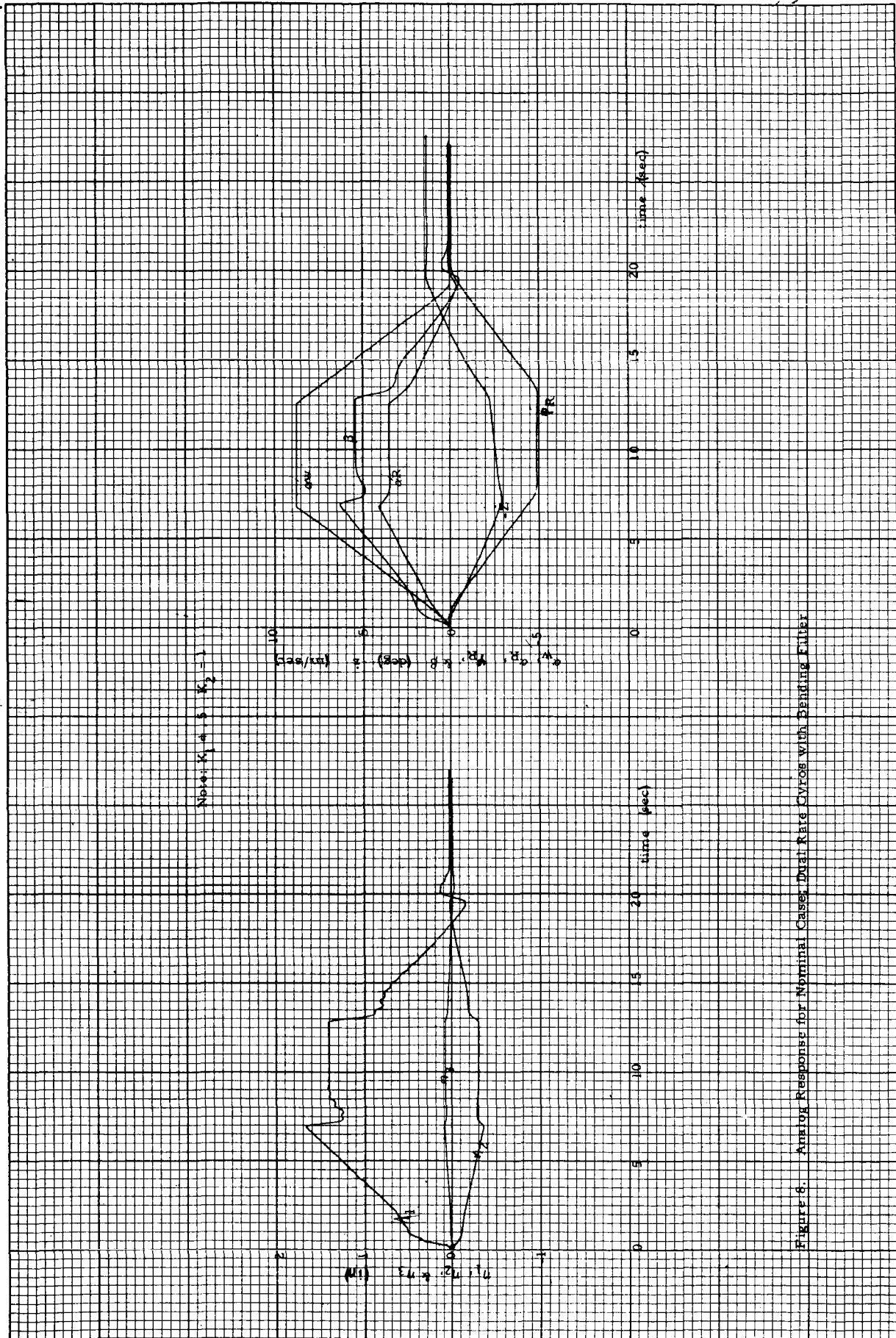


Figure 6. Anisotropic Response for Nominal Cases: Dual Rate Cylinders with Bending Filter

Note: $R_1 = 1$, $R_2 = 1$

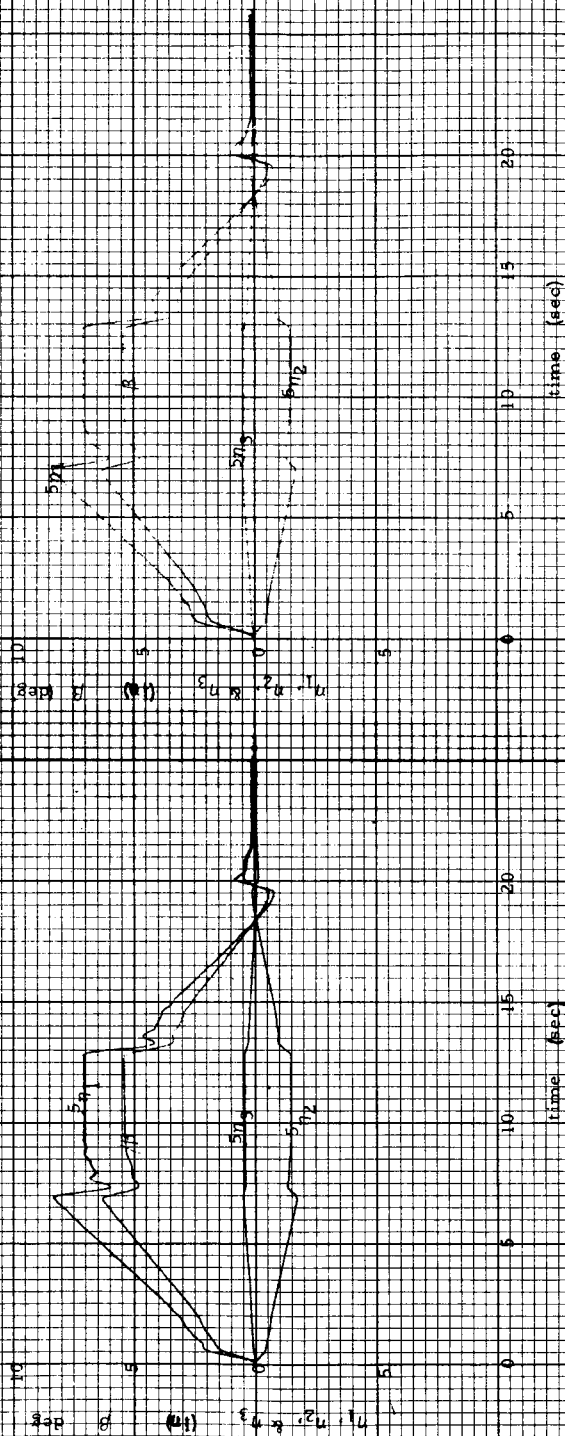


Fig. 9A: 100% Increase in 1st and 2nd Bending Mode Slopes of ± 15

Fig. 9B: 100% Increase in all Bending Modes Slopes of ± 12

Figure 9: Analog Response for 100% Increase in Bending Mode Slopes at Both Rate Gyro Locations

NOTE: $K_1 = .5$ $K_2 = 1$

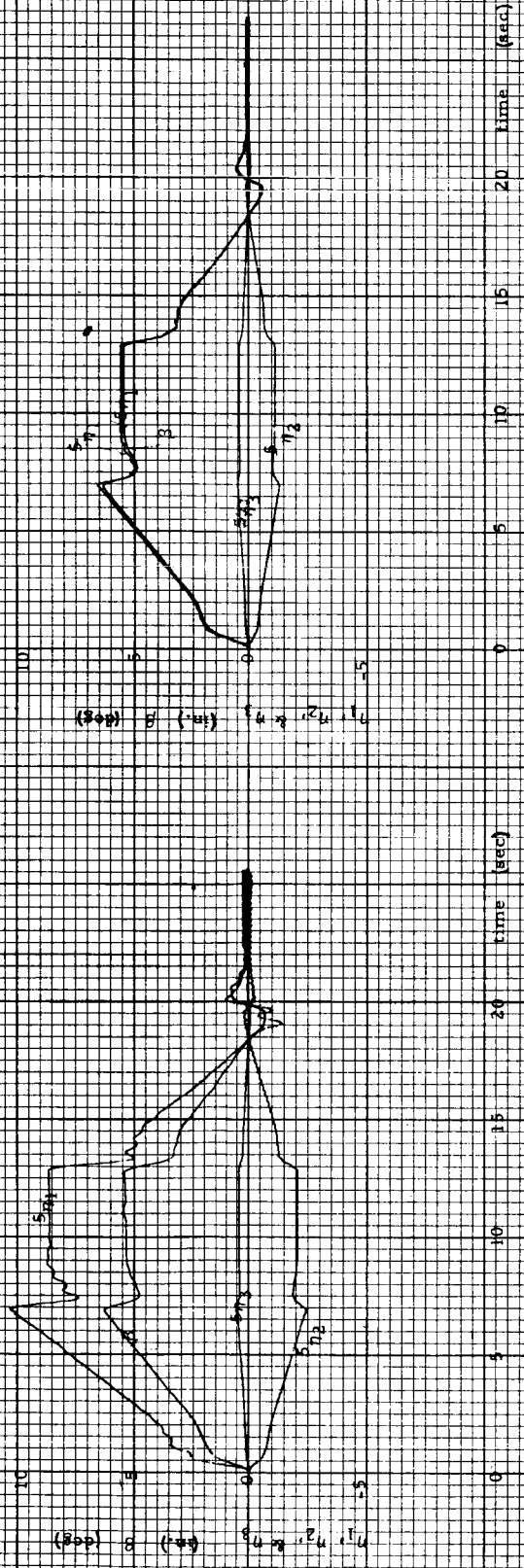


Fig. 10A: ω_n decreased by 10%, ω_d decreased by 15%

Fig. 10B: ω_n increased by 10%, ω_d increased by 15%

Figure 10. Analog Response for $\pm 10\%$ Variations in First Bending Mode Frequency and $\pm 15\%$ Variations in Second Mode Frequency

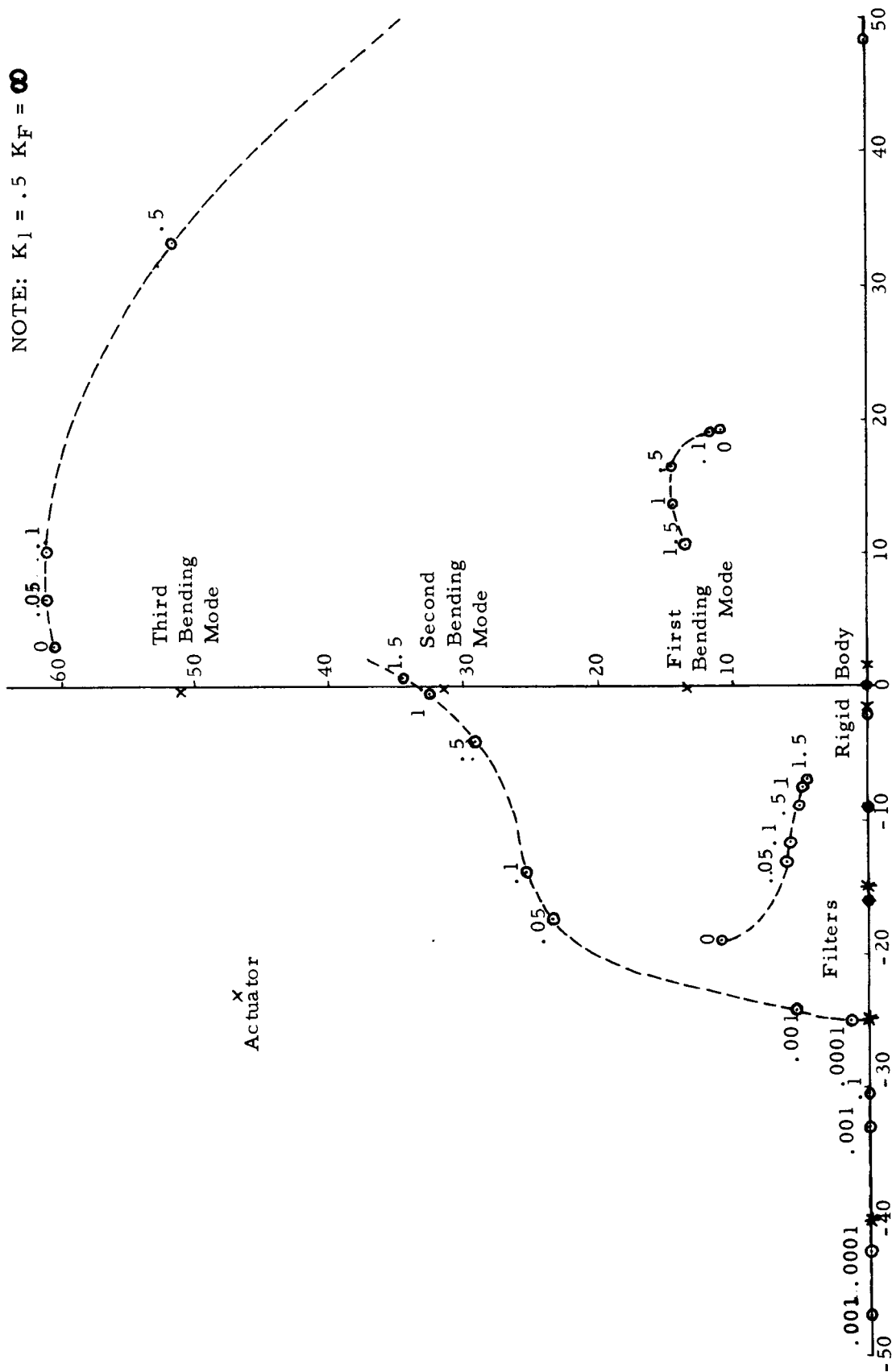


Figure 11: ROOT LOCUS OF CLOSED LOOP ZEROS AS A FUNCTION OF BENDING FILTER SECOND MODE GAIN K_2 .

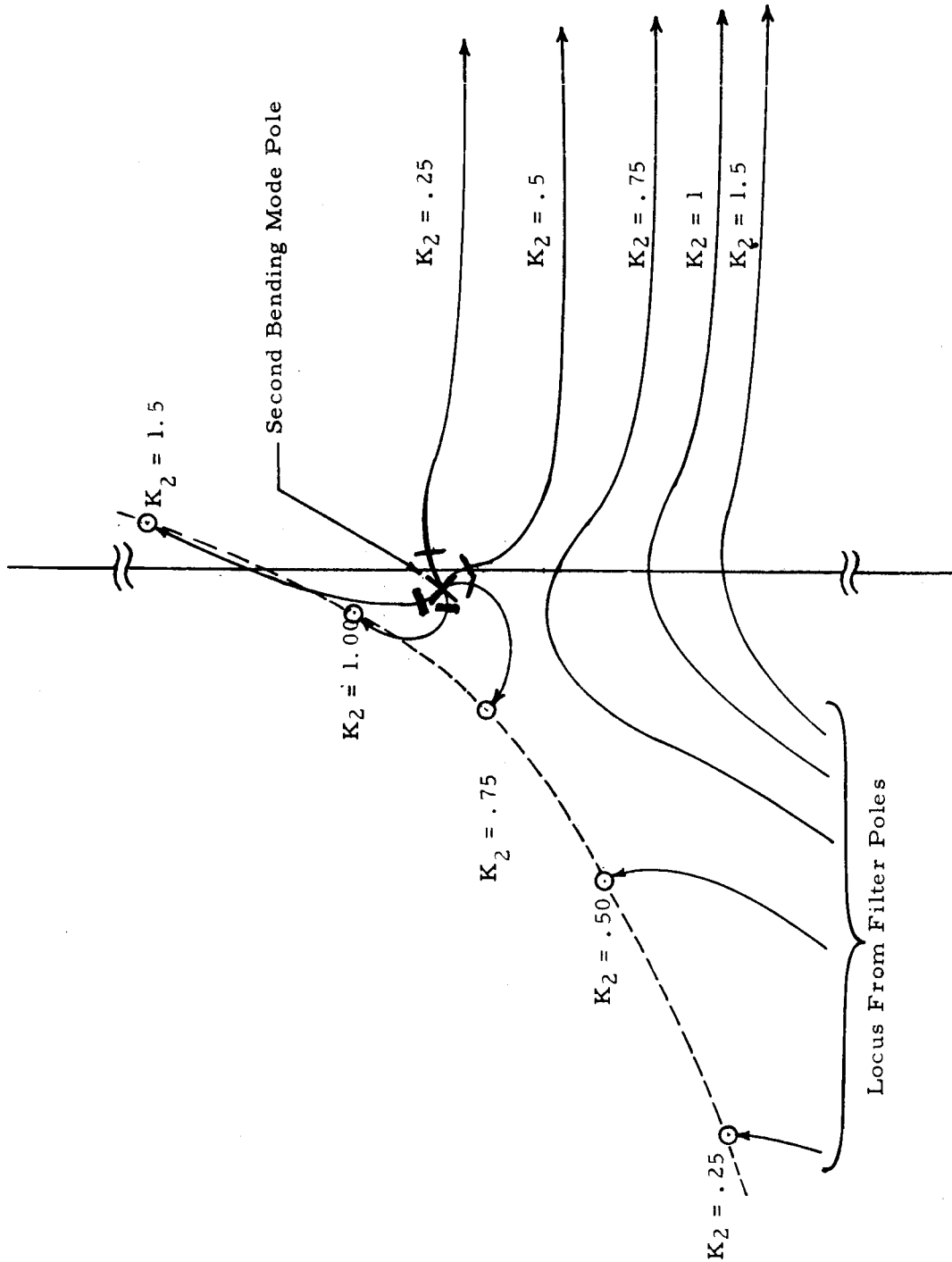


Figure 12: ROOT LOCI NEAR SECOND BENDING MODE FOR SEVERAL VALUES OF K_2

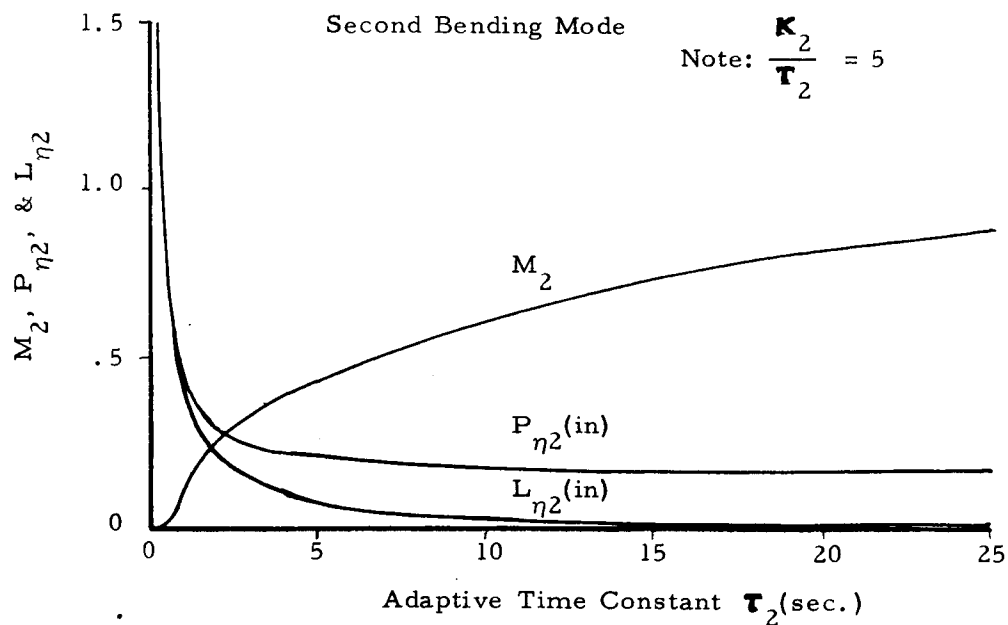
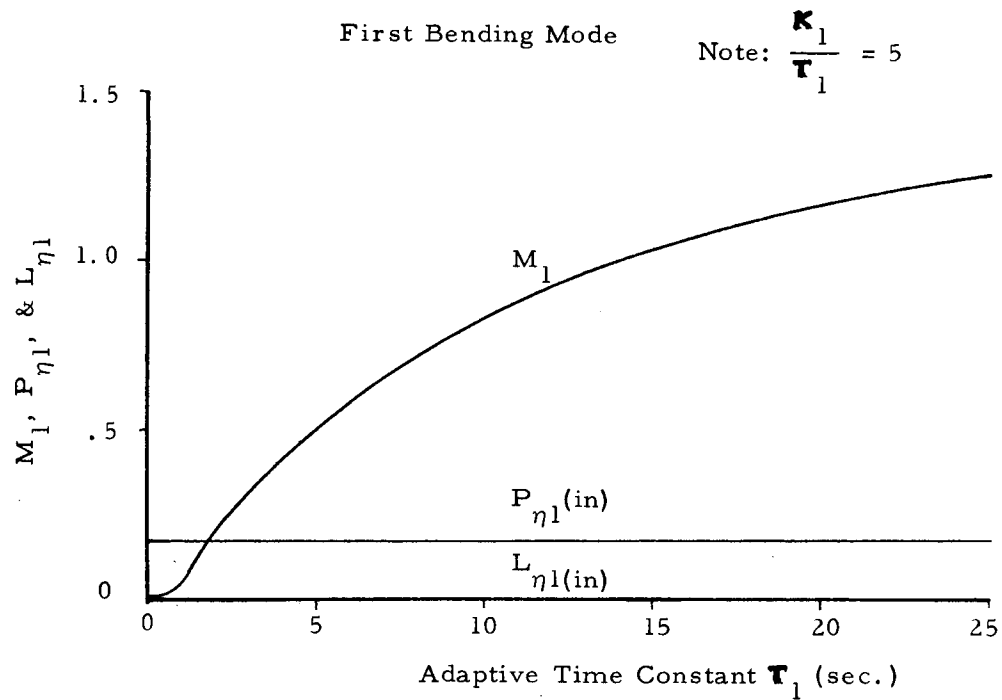


Figure 13: VARIATION OF ADAPTIVE GAIN OVERSHOOT RATIO, MAXIMUM BENDING AMPLITUDE, AND MAGNITUDE OF BENDING LIMIT CYCLE WITH ADAPTIVE TIME CONSTANT.

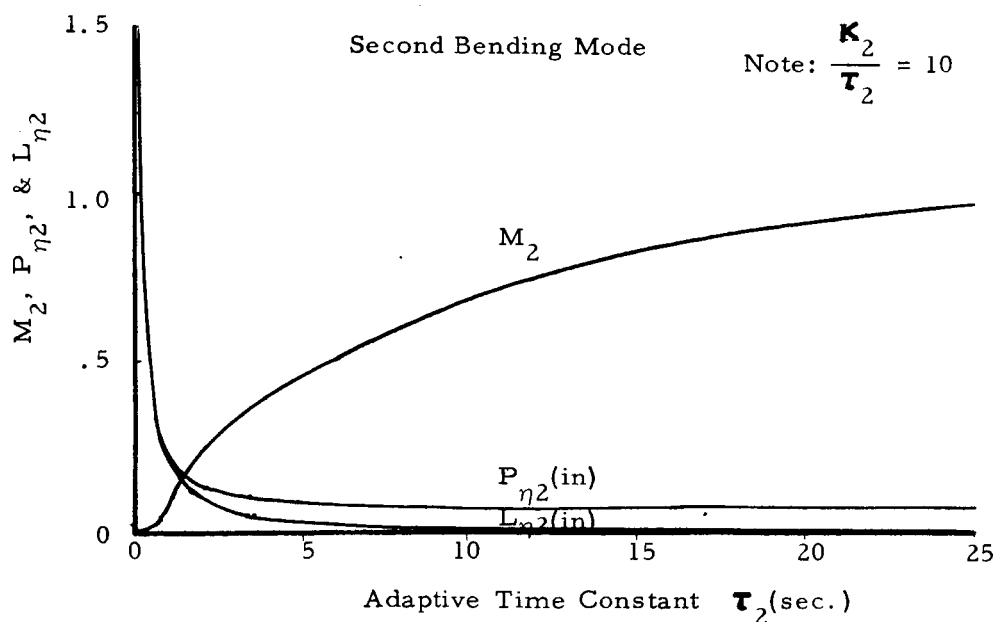
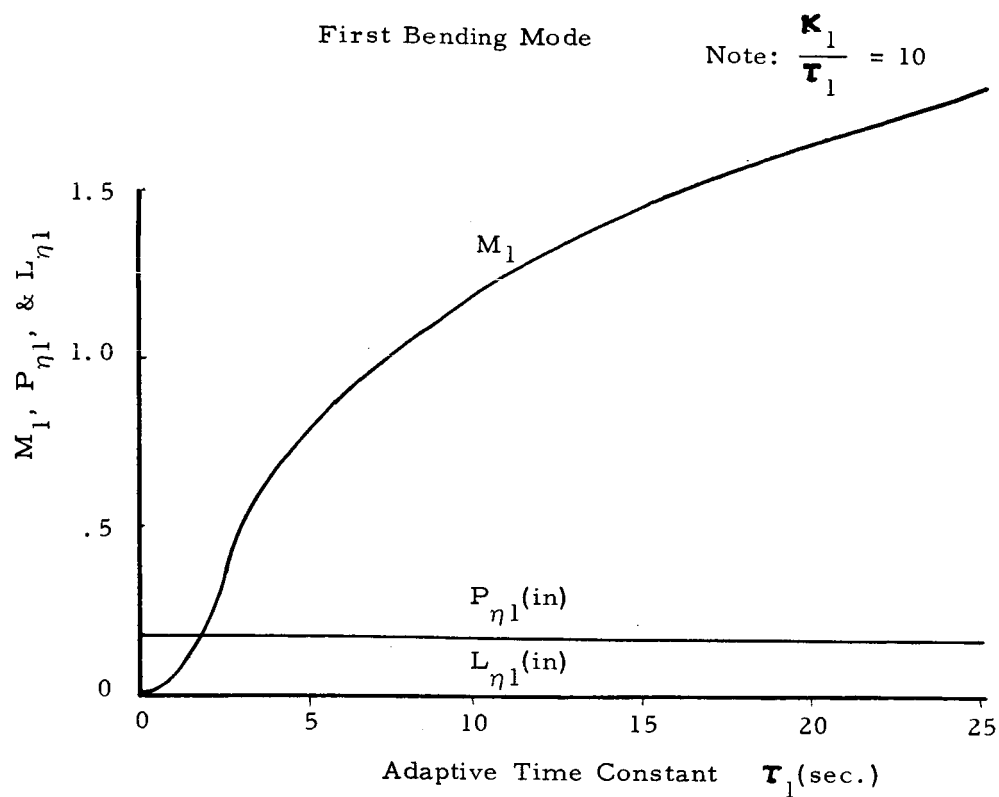


Figure 14: VARIATION OF ADAPTIVE GAIN OVERSHOOT RATIO, MAXIMUM BENDING AMPLITUDE, AND MAGNITUDE OF BENDING LIMIT CYCLE WITH ADAPTIVE TIME CONSTANT.

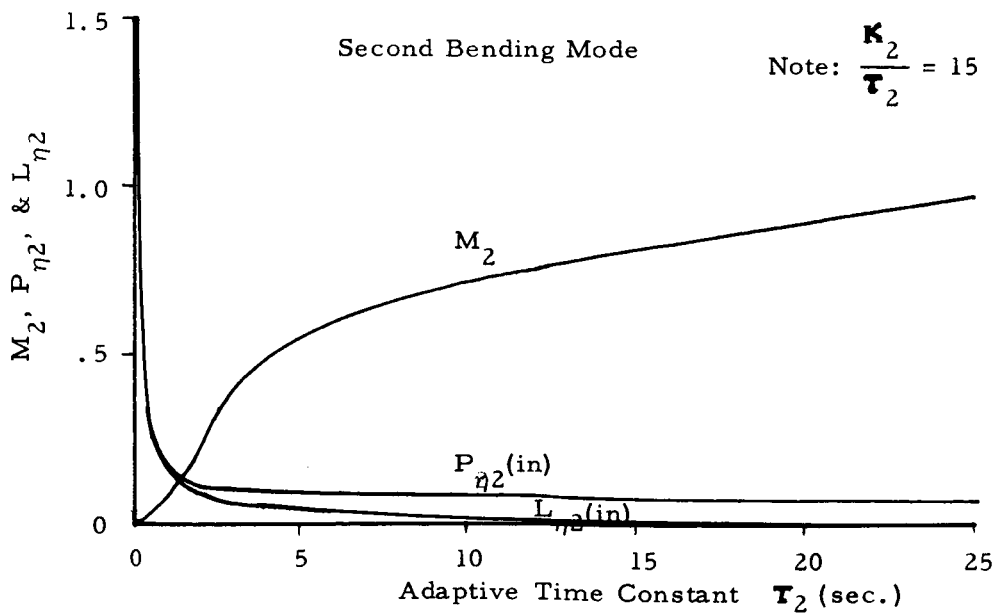
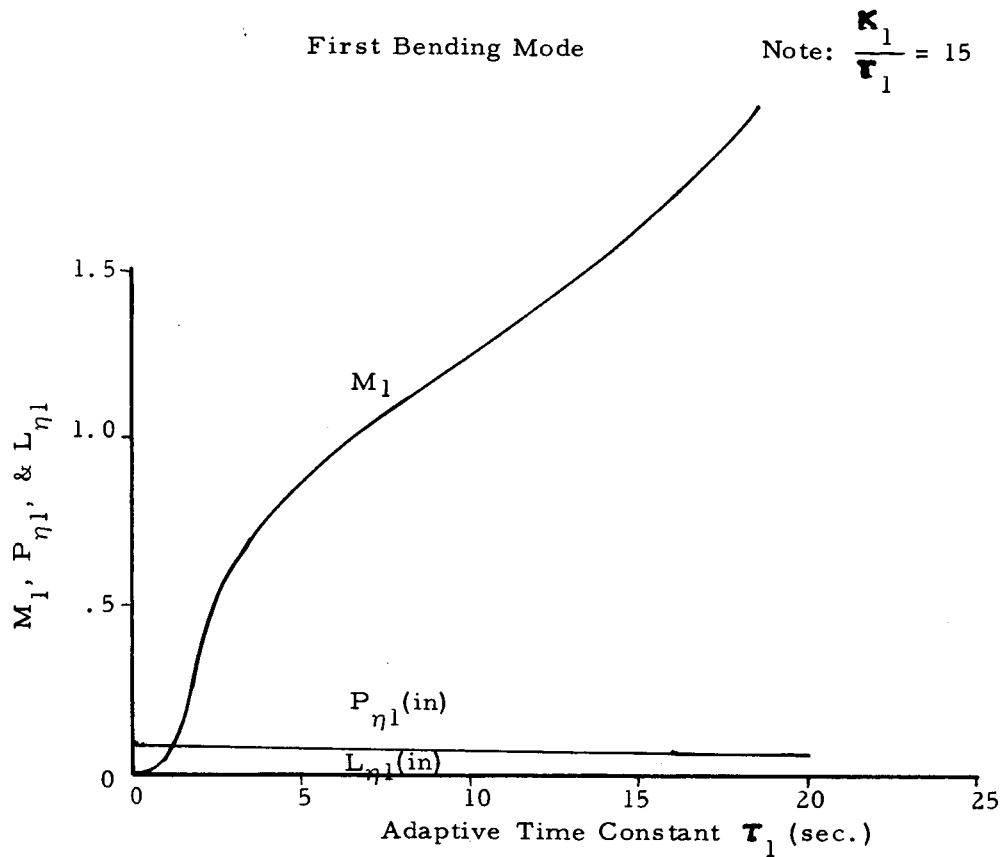


Figure 15: VARIATION OF ADAPTIVE GAIN OVERSHOOT RATIO, MAXIMUM BENDING AMPLITUDE, AND MAGNITUDE OF BENDING LIMIT CYCLE WITH ADAPTIVE TIME CONSTANT.

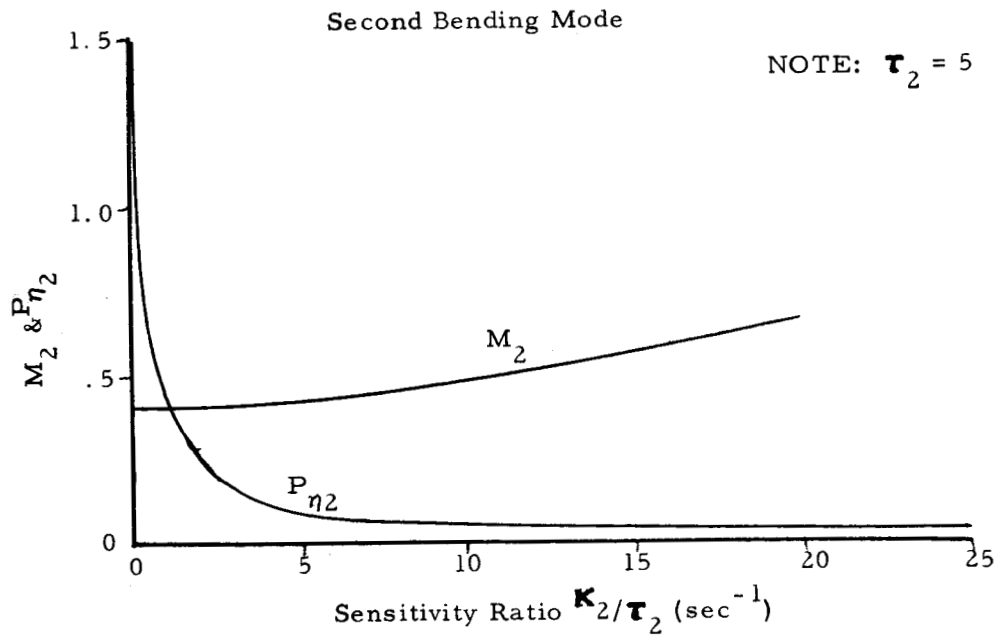
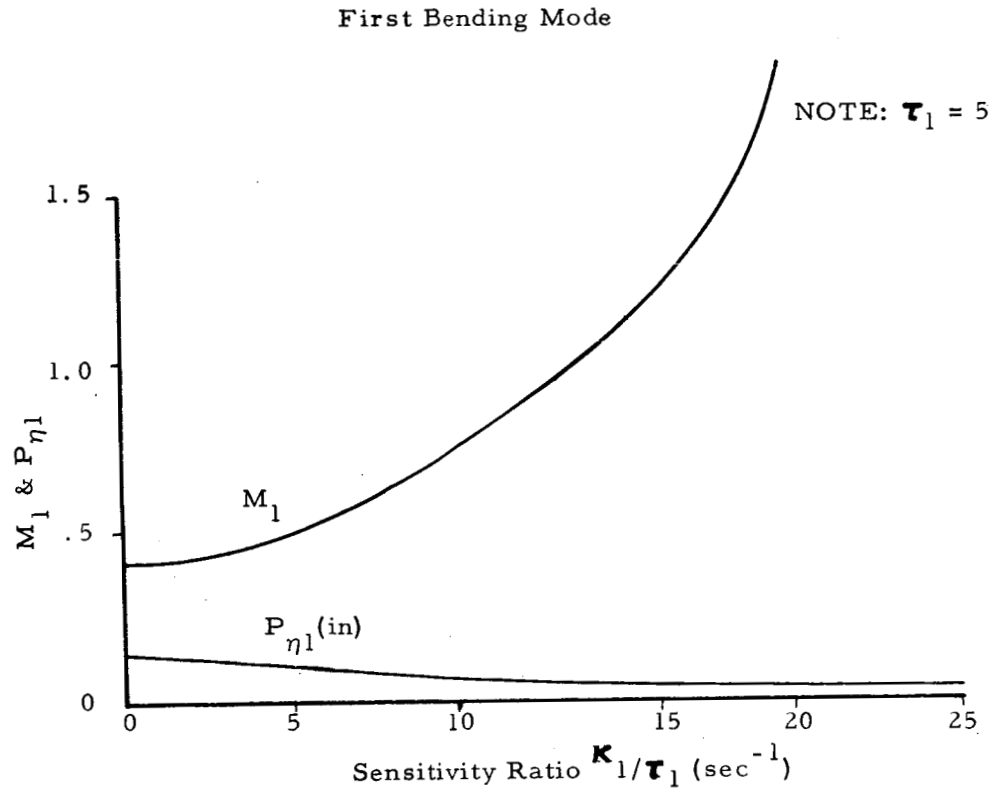


Figure 16: VARIATION OF ADAPTIVE GAIN OVERSHOOT RATIO AND MAXIMUM BENDING AMPLITUDE WITH SENSITIVITY RATIO.

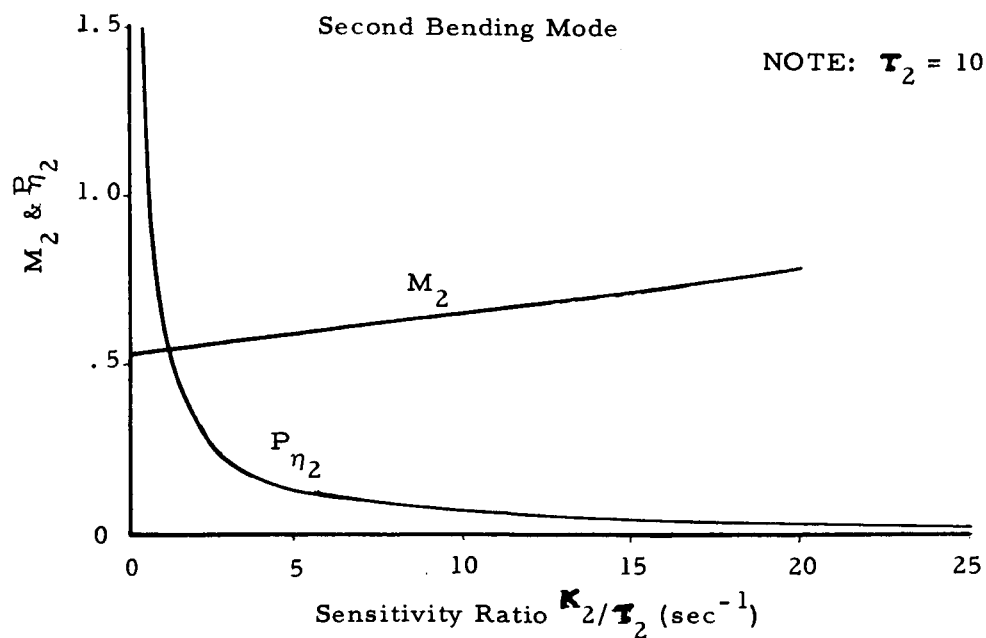
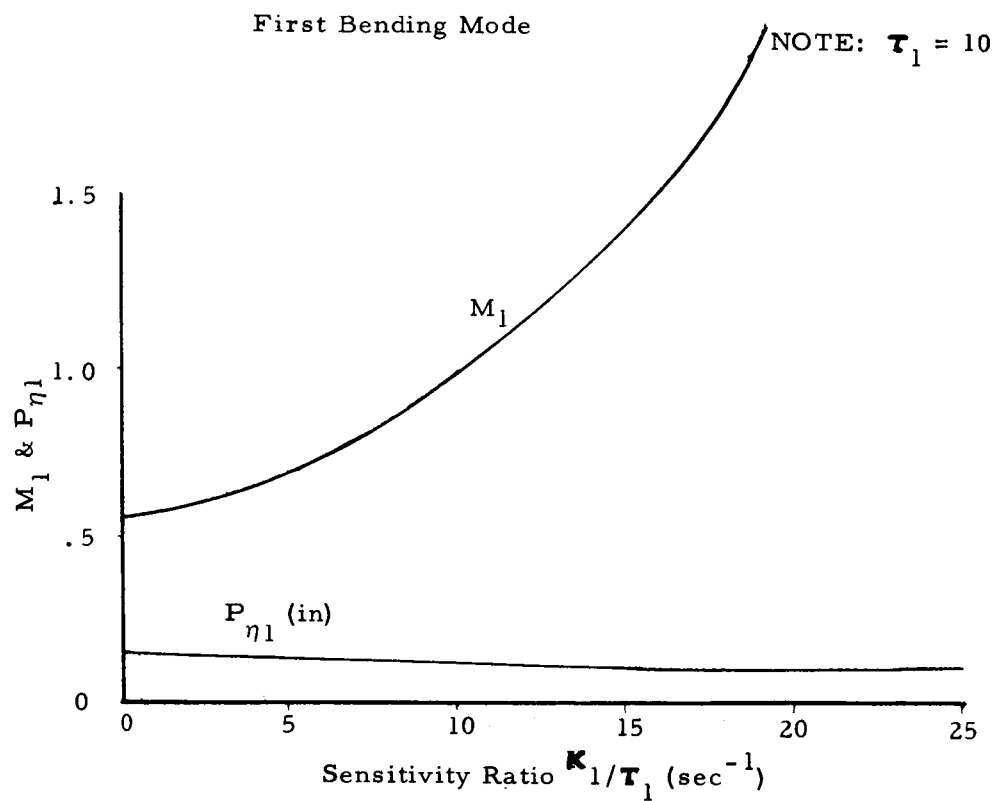


Figure 17: VARIATION OF ADAPTIVE GAIN OVERSHOOT RATIO AND MAXIMUM BENDING AMPLITUDE WITH SENSITIVITY RATIO.

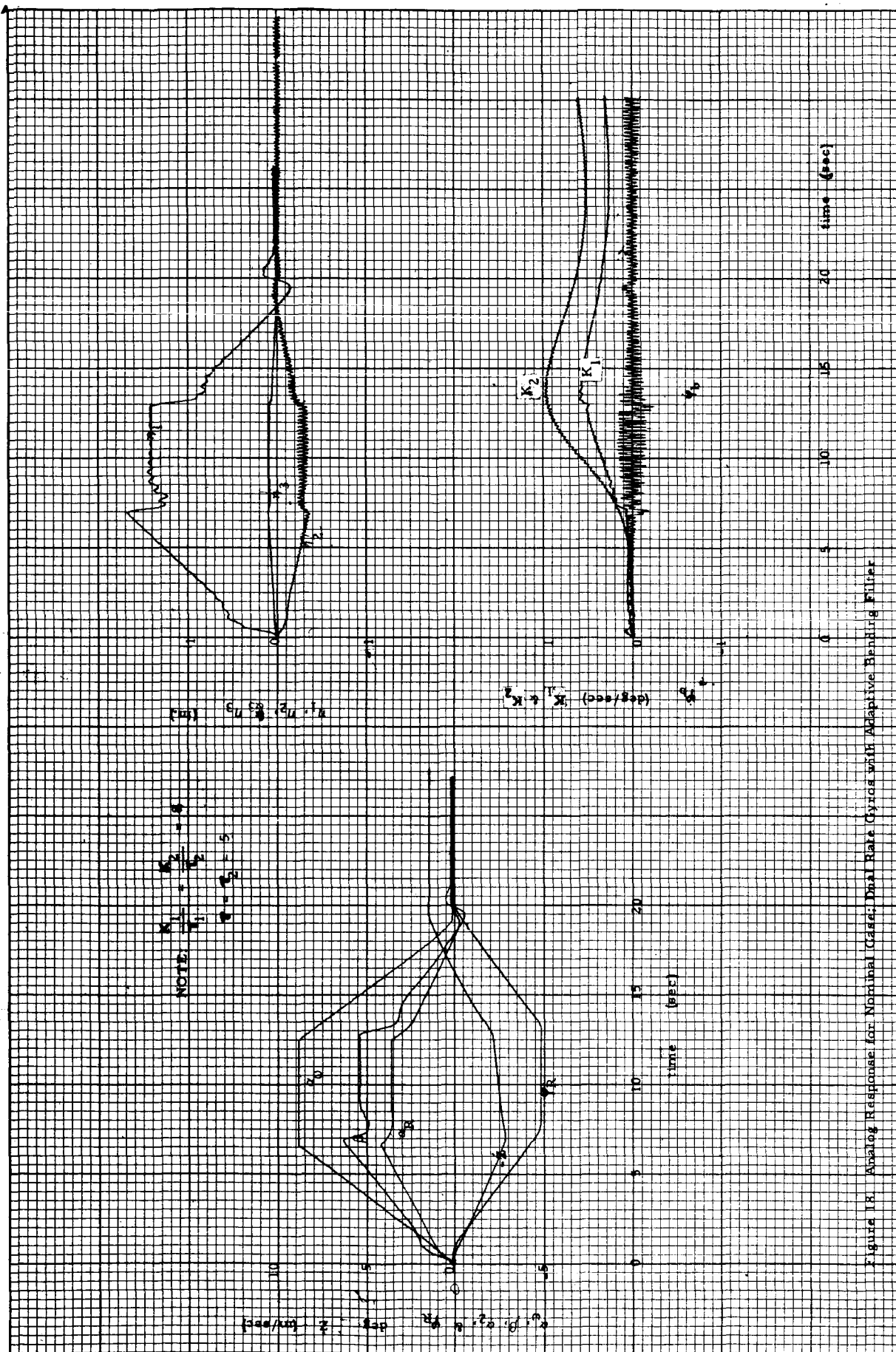


Figure 18. Analog Response for Nominal Case; Dual Rate Cycles with Adaptive Bending Filter

NOTE: $\frac{R_1}{R_2} = 1$, $\frac{R_1}{R_2} = 1$, $\frac{R_1}{R_2} = 1$



Figure 19. Analog Response for 100% Increase in First and Second Bending Mode Slopes at Both Rate Gyro Locations; Aspirin Bending Filter

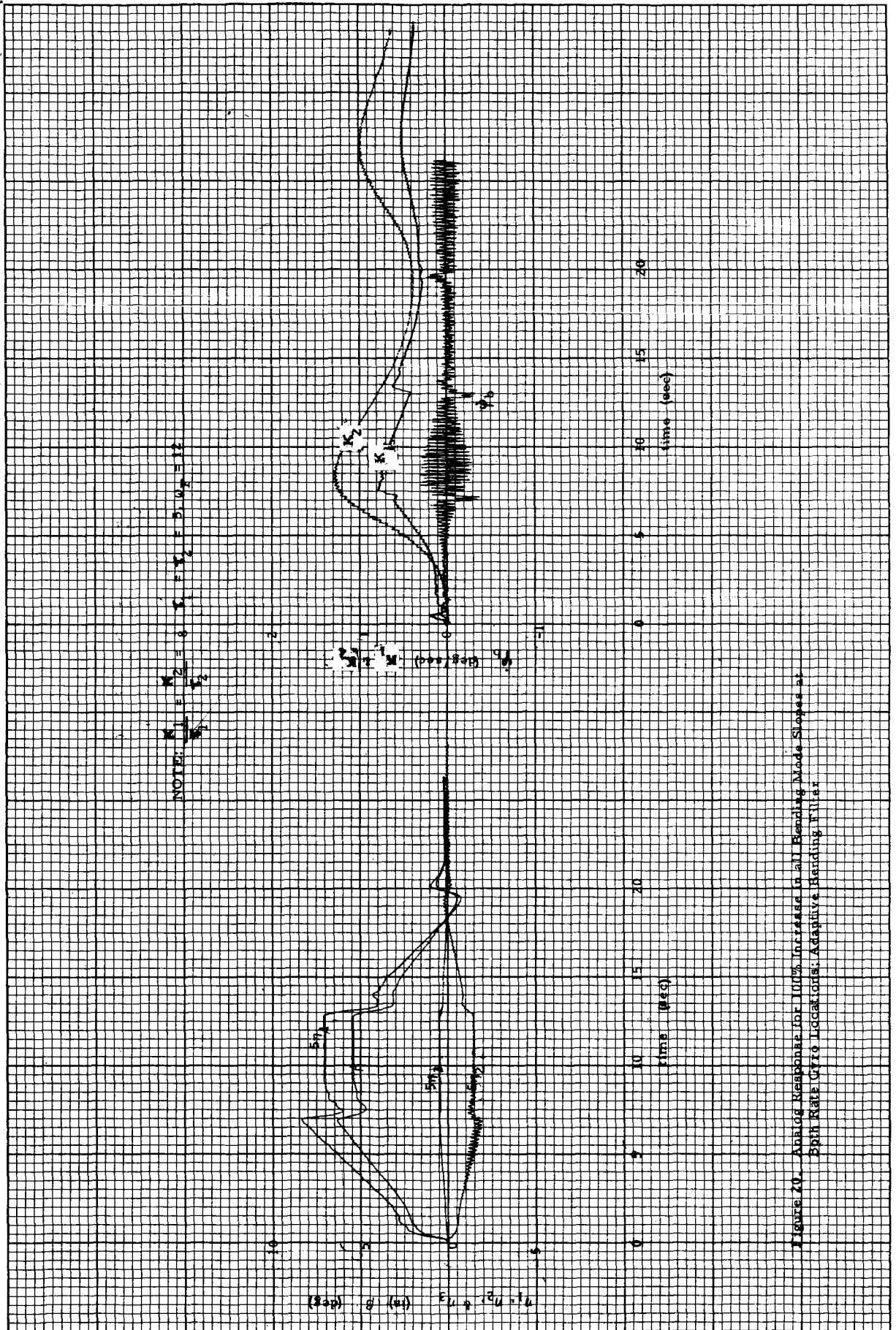
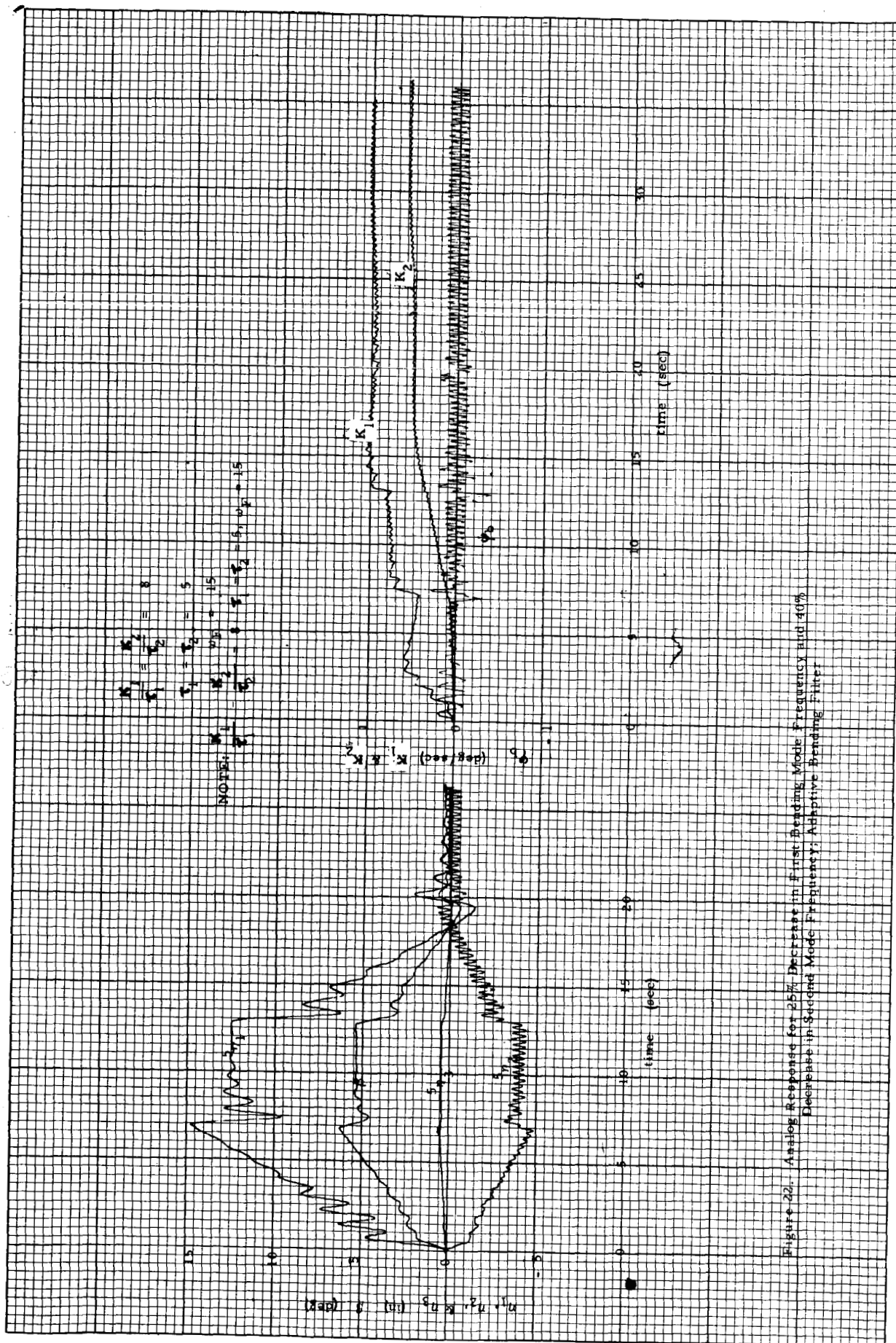


Figure 20. Analog Response for 100% Increase in all Bending Mode Slopes at Both Rate Of Locations: Adaptive Banding Filter.

NOTE: $\frac{K_1}{K_2} = 8$ $\frac{K_1}{K_2} = 5.0$ $\frac{K_1}{K_2} = 13$



Figure 21: Analytic Response for 25% Increase in First Banding Mode Frequency and 65% Increase in Second Mode Frequency; Adaptive Banding Filter



APPROVAL

MTP-AERO-63-21

A DUAL RATE GYRO APPROACH TO
THE ELASTIC FEEDBACK PROBLEM

ROBERT C. LEWIS

and

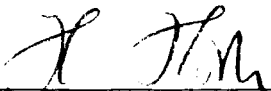
THOMAS E. CARTER

This information in this report has been reviewed for security classification. Review of any information concerning Department of Defense or Atomic Energy Commission programs has been made by the MSFC Security Classification Officer. This report, in its entirety, has been determined to be UNCLASSIFIED.



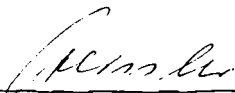
CLYDE D. BAKER

Chief, Trajectory Shaping & Special Missions Section



HELMUT J. HORN

Chief, Dynamics Analysis Branch



E. D. GEISLER

Director, Aeroballistics Division

DISTRIBUTION

M-ASTR

Mr. Hosenthien
Mr. Moore

M-AERO

Dr. Geissler
Dr. Hoelker
Mr. Horn
Mr. Dahm
Mr. Baker
Mr. Golmon
Mr. Rheinfurth
Mr. Stone
Mr. Hart
Mr. Ryan
Mr. Thomae
Mr. Linsley
Mr. Winch
Mr. Callaway
Mr. Cummings
Mr. O. C. Jean
Mr. Braunlich
Mr. McNair
Mr. Lovingood
Mr. Lindberg
Mr. Mowery
Dr. Ford
Mr. Vaughan
Mr. Scoggins
Mr. Lewis (15)
Mr. Scoggins (15)

M-MS-IP

M-MS-IPL (8)

M-MS-H

M-PAT

M-HME-P

Scientific and Technical Information Facility (2)
Attn: NASA Representative (S-AK/RKT)
P. O. Box 5700
Bethesda, Maryland